Msc Thesis

Martian Gale crater methane as a potential biosignature for anaerobic communities: an experimental bayesian approach

Dylan D. Verburg

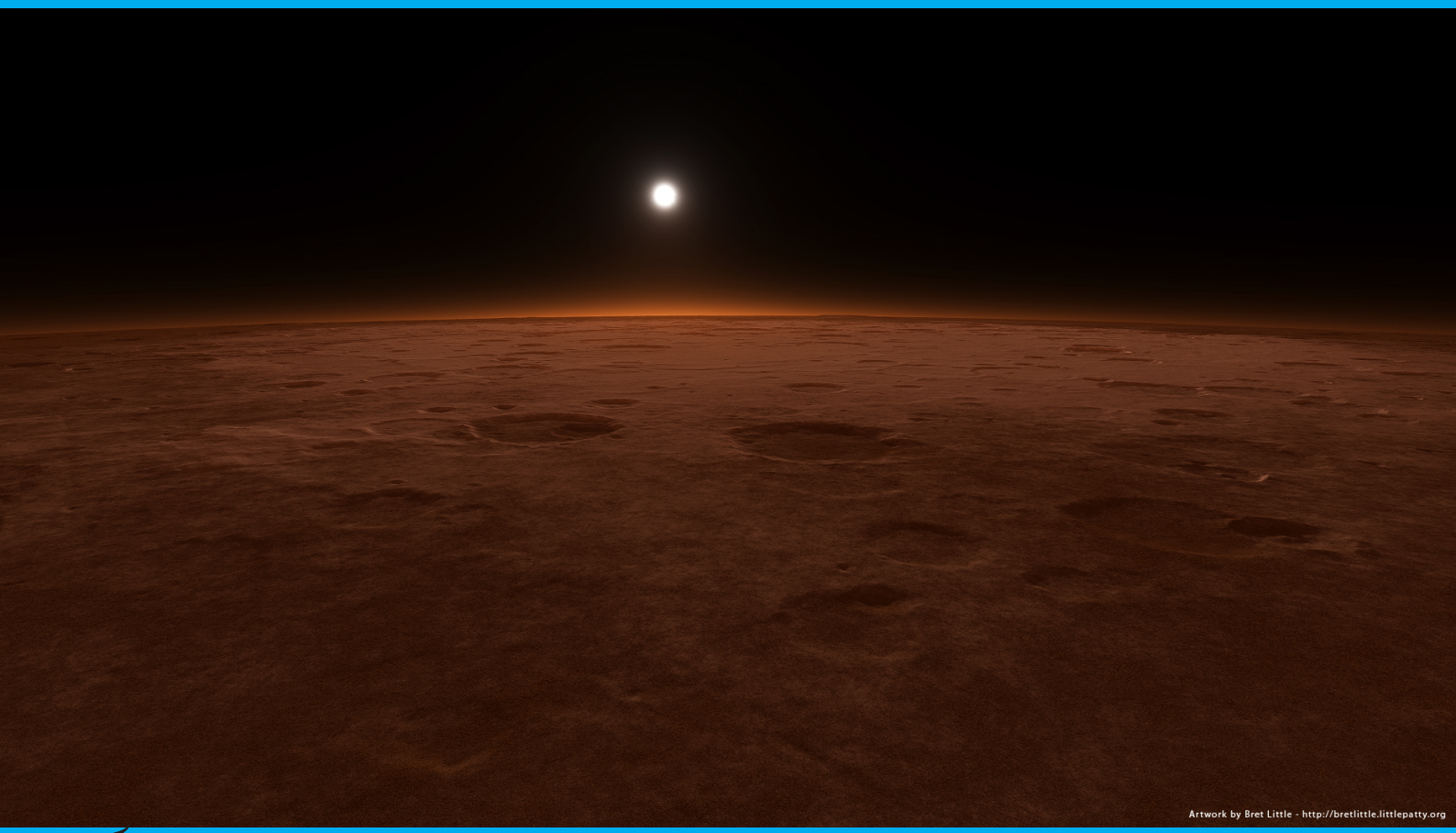

Artwork by Bret Little - http://bretlittle.littlepatty.org

TU Delft

Msc Thesis

Martian Gale crater methane as a potential biosignature for anaerobic communities: an experimental bayesian approach

by

Dylan D. Verburg

Student Name	Student Number
D.D. Vebrurg	4976797

to obtain the degree Master of science
at the Delft University of Technology,
to be defended publicly on March 30 2023, at 15:00.

Assessment committee	
Chair:	R.E.F. Lindeboom
2nd assessor:	J.B. van Lier
3rd assessor:	J. Gebert

Cover: Artwork by Bret Little - http://bretlittle.littlepatty.org

TU Delft

Acknowledgement

I want to thank Kristel Mijnendonckx from SCK-CEN for supplying the organisms and boom clay sample used in my experiments. Also, I would like to express my gratitude for answering all my questions regarding the microorganisms. I would also like to thank Jo Slijpen from Sibelco for providing the minerals I used in the Martian regolith analogue.

I am very grateful to my friends and family who took the time to help me write this document and tolerated my monologues on its contents.

Lastly, I would not have been able to perform my experiments without the help of the Waterlab staff at TU Delft.

Abstract

On the 14th of July 2013, a methane peak was observed in the Gale crater. This methane peak has been investigated in a non-biological context before. This study applies exoplanet research strategies and knowledge about biological methane production on Earth to investigate the biological context. Bayes formula is the foundation of the Bayesian framework approach as proposed by Walker et al. [53]. This Bayesian framework allows for separate investigation of biotic and abiotic methane production pathways to assess the likelihood that one of these pathways is responsible for the methane observation.

Before probability is investigated, the viability of biotic methane production is gauged by Thermodynamic calculations. These calculations use the Gibbs free energy and show methanogenesis and sulfate reduction as viable catabolic reactions under Martian temperature and chemical soil and atmosphere compositions. Mars analogue Experiments were conducted into the kinetics of methane and hydrogen sulfide gas production under the influence of Martian Regolith analogue and Martian atmospheric analogue. The seed organisms were gathered from the Belgian Boom clay layer in the HADES lab because the Boom clay layer has strong mineralogical similarities to the Martian regolith. The experiments show that both methane and hydrogen sulfide gas production is not significantly affected by the introduction of modified Phylosilicate Martian Regolith Analog (P-MRA) and Martian Atmosphere Analog (MAA). Comparison with the ADM1 kinetic model shows that only methane gas production is comparable within one standard deviation between all experiments and the model. Biomass growth and sulfur gas production are inconsistent between experiments and the kinetic model. To quantify the probability of biotic methane production, a modified ADM1 model was used for Monte Carlo (MC) analysis of the correlation between the Martian observed methane peak and the kinetic model output for varying initial chemical conditions and virtual reactor volumes. Based on this, 78% of the simulations showed a significant correlation. Using Bayes formula, the posterior probability of the methane peak being biological in origin is higher than the prior probability of an anaerobic community being active around the Gale crater. However, this misses the crucial information on the chance of this methane peak occurring in abiotic conditions.

Contents

Nomenclature

ΔG^0	Change in Gibbs free energy at standard conditions
ΔG^0_{Tx}	Change in Gibbs free energy at standard pressure and non-standard temperature x
$\Delta G^1_{T,P}$	Change in Gibbs free energy at pressure P and temperature T
ΔH^0	Enthalpy at standard pressure and temperature
$P(CH_4 \mid life)$	conditional probability of observing methane given life is present
$P(CH_4 \mid nolife)$	conditional probability of observing methane given no life is present
$P(life \mid CH_4)$	Posterior probability of observing life given methane is observed
$P(life)$	prior probability of that life is present
$P(X \mid Y)$	The conditional probability of X given Y was observed
P_x	Partial pressure of component x
Abiotic	Not biological
ADM1	Anearobic Digestion Model number 1
Biotic	Biological in origin
Boom clay	Inorganic clay formation under Belgium and part of the Netherlands
COD	Chemical Oxygen Demand, the amount of oxygen theoretically needed to fully oxidize a sample [g O_2 / L]
hSRB	hydrogenotrophic Sulphate Reducing Bacteria
Life	Active organic methane-producing microbial community
MAA	Martian Atmospheric Analog
MC	Monte Carlo
MCMC	Monte Carlo Markov Chain
MRA	Martian Regolith Analog
P	Pressure
P-MRA	Phylosilicate Martian Regolith Analog
RMSE	Root Mean Square Error
TSS	Total Suspended Solids
VSS	Volatile Suspended Solids, often used as an approximation for biomass

1

Introduction

On the 14th of June 2013, the Curiosity rover measured a peak in trace methane on the Martian surface (figure 1.1) in the Gale crater [21]. This observation was confirmed by the Planetary Fourier spectrometer aboard the Mars Express satellite. The Martian atmospheric lifetime of methane is 340 years, making any methane in the atmosphere geologically recent emissions [30]. The atmospheric mixing time on Mars is only six months; observing a local peak in trace gasses means that the emission is less than six months old [54].

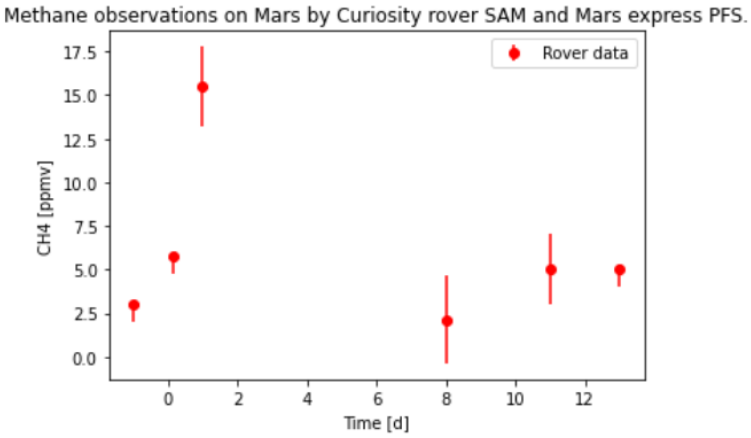

Figure 1.1: The methane peak measurements from sol 304 (the 14th of June 2013) onward [21]. This methane peak forms the Martian data, substantiating the search for possible life. The axact values can be found in table 2.3

By definition, Martian methane was produced either biologically or non-biologically. Most research into the Martian methane peak has so far focused on non-biological production [29] [30] [5]. While valuable, this leaves a knowledge gap in the biological hypothesis. On Earth, most methane is produced biologically by anaerobic organisms called methanogens [44]. These methanogens live in a wide range of anaerobic locations, including the deep subsurface, near subsea hydrothermal vents and in the gastrointestinal tract of mammals [24] [35]. Methanogens are well understood on Earth and are speculated to be one of the oldest living organisms together with sulphate reducers, based on the chemical reactions in lost city type hydrothermal vents [35]. This age is reinforced by genetic analysis via the last universal common ancestor theory [35]. The assumption that methanogens and sulphate reducers are closely related to the first forms of life plausible. Given this assumption, early life formed on Mars would likely also be closely related to methanogens or sulphate reducers. These potentially ancient organisms coexist and compete with each other and an entire biosphere of other anaerobic organisms in nature on Earth. Given the evolutionary evidence for the diversification of life over time, it is unlikely that life on other planets consists of a single organism, provided enough time has passed to allow evolutionary diversification. Therefore, biological methane production in a mixed culture will be the focus of this study.

Due to the complexity of Martian measurements and associated uncertainty in attributing any single measurement to methane-producing life, the methane cannot be clearly attributed to any biological process. The solution to this uncertainty is a structured analysis of both non-biological and biological processes using a proposed 'Bayesian framework'. In this framework, ' bio signatures' are not seen singularly, but in context to each other, environmental factors and other observations [53]. This framework is used in exoplanetary research to assess potential 'biosignatures systematically'. These biosignatures are characteristic evidence for life, while a potential biosignature is not final proof of past or present life.

The Martian methane peak is such a potential biosignature. It can thus be investigated within the Bayesian framework by quantifying the two opposing hypotheses and the prior probability of life (P(life))via equation: 1.1. In that equation, C_i denotes additional observational variables, such as observing an H_2S peak when a methane peak is observed. The Martian methane peak was either produced biologically (biotic) or produced by thermochemical water gas reactions (abiotic). These two possible pathways based on terrestrial knowledge and within the formula are denoted by $P(CH_4|life, C_i)$ and $P(CH_4|nolife, C_i)$. In the context of the structured search for life, constraining the biotic likelihood is a first step in constructing the Bayesian framework [53].

$$P(life|CH_4) = \sum_i \frac{P(CH_4|life, C_i)P(life, C_i)}{P(CH_4|life, C_i)P(life, C_i) + P(CH_4|nolife, C_i)(1 - P(life, C_i))} \tag{1.1}$$

However, the current state of the art views potential biosignatures as binary, either existing or not existing [53]. The chance only describes the likelihood of correct detection. This study aims to quantify the chance of biotic production being responsible for the peak by proposing a novel method of kinetic comparison between a mechanistic model of known biotic methane production and the Martian observations. This method allows the Bayesian framework to be quantified and provides a method to compare future observations against. Contrary to the data available for the exoplanetary research Walker et al. [53] focus on, Martian data's temporal and spatial data resolution is much higher. This high data resolution allows the dynamic analysis to be conducted. This altered method of investigating dynamics instead of presence is also described as a possible future step in astrobiological inter-disciplinary research [53].

This approach poses the opportunity to populate the Bayesian framework with dynamic findings and verify them via in-situ methods. In-situ verification is possible due to the astronomically speaking short distance between Earth and Mars. The dynamic analysis sheds light on how life on other worlds could function and the viability of the dynamic process to investigate biosignatures.

This study aims to find the chance that Earth-like life was responsible for the methane spike around sol 305 (the 14th of June 2013) and express this in a percentage. Consequently, this study will also explore what this form of life could be. This study is conducted under the hypothesis that life on Mars exists and is similar to life on Earth. This assumption is substantiated in chapter 2.

2

Literature review

2.1. Introduction

The research question is: How likely, in percentages, is it that the methane detected in the Martian Gale crater can be attributed to one or more Earth-like organisms? This question flows from the more basic question of finding the cause of the methane measurements on Mars. It is important to note that the research question focuses on the methane spike as a potential biosignature. There exist two fundamental explanations for the methane spike. Either the methane was produced biologically or abiotically. The Bayesian framework allows these two hypothesis to be weighed against each other. The hypothesis of life-mediated methane production will be investigated in this study, providing half of the contents of the Bayesian framework. The framework, together with how the variables will be quantified, is in figure 2.1.

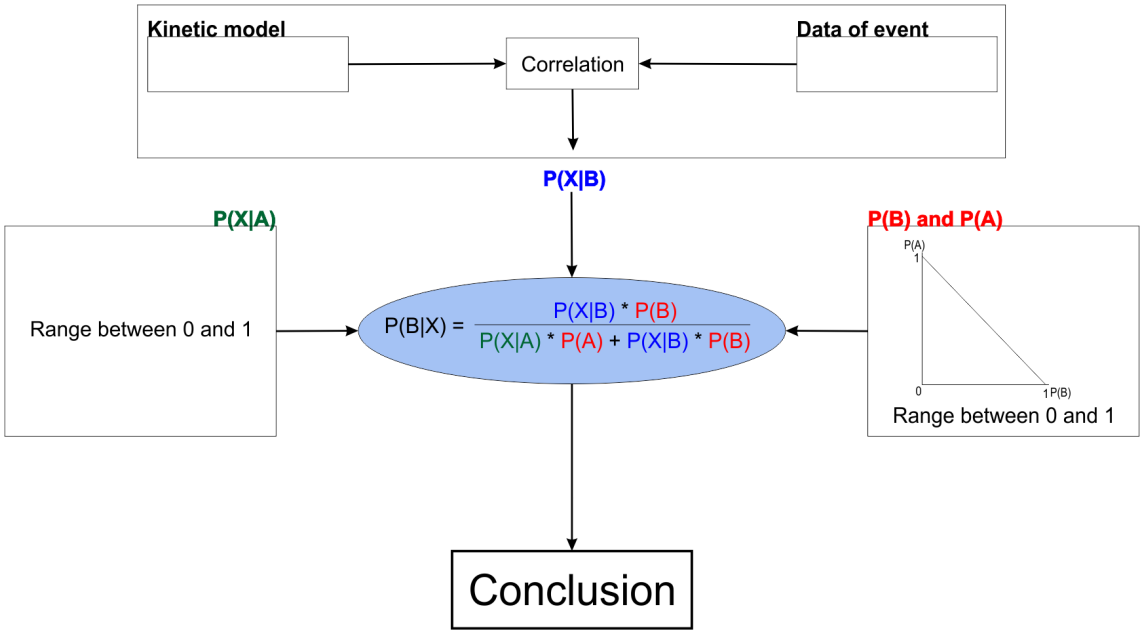

Figure 2.1: Overview of road map from raw data to a conclusion. The constraints of $P(life)$ are explained in chapter 2, with the knowledge that $P(life)$ and $P(nolife)$ are mutually exclusive. The correlation between model output and real-world observations is found by employing a Pearson correlation. This method provides a value for $P(CH_4|life)$ via the method in 3.3.

The research question will be investigated using the questions posed by Catlin et al. [7] to structure the investigation. These questions are postulated to facilitate a structured analysis of potential biosignatures within their context for exoplanetary research. These questions are listed as the subsections of this chapter to facilitate a structured literature study into the context of the Martian methane spike. This investigation will slightly change the questions posed by Catlin et al. [7], focusing on finding constraints for the factors of equation 2.1, as well as attempting to find conditions for further constraints. The characterisation of the bio-signature topic

will be expanded by: identifying earth analogue organisms, assessing them thermodynamically, and subsequently investigating their kinetics. This scheme allows the Mars data and Earth analogue to be temporally compared.

2.2. Stellar properties

Stellar properties are properties of the star a planet is orbiting. These will be discussed in general, and how this affects Mars's habitability. In this part, stellar properties are expanded by planetary properties.

2.2.1. General properties

The stellar properties of the star that Mars is orbiting are identical to Earth, as these two planets orbit the same star. This identical star, combined with the cosmically close distance between Mars and Earth, improves the constraints that can be placed on $P(Life)$. As it is generally accepted that life exists on Earth, the chance of life emerging in this solar system is proven non-zero. Note that this does not imply that life originated on Earth but only assumes that it must have 'emerged' at some point in time. The small distance between Earth and Mars improves the chance of life existing on Mars via the theory of panspermia. Life could be carried from Earth, or a different body, to Mars by meteorites [11]. These points imply that life emerging on Earth and emerging on Mars would be similar, either because of the panspermic common ancestor or because of the stellar conditions. Both Earth and Mars were in the sun's habitable zone, further allowing historical co-evolution [18]. The habitable zone is the space around a star where incoming radiation supports surface liquid water. This habitable zone analysis neglects planetary effects on the presence of (liquid) water.

2.2.2. Martian factors affecting habitability

Habitability is the property of a planet to support life if it were there. However, habitability commonly means: stable liquid water at the surface. It can be expanded to mean any place where life can thrive, as is the case in this paragraph [44]. Here factors that could affect habitability on Mars compared to Earth will be discussed. These are: gravitational potential, radiation and temperature differences. The lack of liquid water and the different chemical composition of the atmosphere and regolith are also discussed.

The different gravitational acceleration is an important factor on Mars that could affect simple organisms. The acceleration is around $3.7 m/s^2$ on Mars, while the gravitational acceleration on Earth is $9.81 m/s^2$ [23]. Effects on microbial life can range from slightly altered growth kinetics to different gene expressions [40]. This means some Earth-like organisms could exist without problems, but some would not be viable. In between would be a range where these organisms could exist but behave fundamentally differently. Additionally, the transport of chemicals in the liquid phase is affected by the formation of a 'thin film'. This film occurs between solids and bulk liquids. The decreased gravitational potential increases the' thin film' thickness, negatively affecting the chemical transport towards the microbe [50].

The lack of a magnetosphere, and the much thinner atmosphere, fail to prevent high energy radiation and high energy particles from reaching the surface of Mars [22]. This increased burden on microbial life could have a large negative impact on habitability at the surface but less so at depth. This impact was found for both ionising radiation and UVC radiation, albeit the UVC exposure survivability was in terms of hours. The survivability for ionising radiation was half a million years for dormant cells instead of functioning ones [45][9]. Simply put, the effect of UVC is deadly, while for ionising radiation, this is survivable. Microbes could sustainably survive in an irradiated environment, but they cannot do this in an environment with UVC radiation. The regolith can shield against incoming high-energy particles and (ionising) radiation, provided the column is large enough. The radiation effects imply that life would likely be underground.

The diurnal and seasonal temperature fluctuations on Mars pose another threat to potential life. On Mars, the surface temperatures can vary between roughly 191K up to 294K [25]. No subsurface outliers are expected based on thermal measurements by the Mars Odyssey orbiter [30]. This temperature range can have a profound negative effect on habitability. Specifically for methanogens, this diurnal cycle can greatly affect gas production, and survival [37]. Habitability is closely related to liquid water, which would be scarce at these temperature ranges. Sub-zero Celsius temperatures, however, do not exclude life as long as the water occasionally liquefies [41]. This fact is further reinforced by arctic microbes being able to survive freeze-thaw cycles [31].

While not affecting habitability, the diurnal temperature fluctuations on Mars, in combination with the presence of an atmospheric boundary layer, effects gas detection. The atmospheric boundary layer could cause nighttime containment of methane [55]. As the ground cools, the atmospheric boundary layer lowers,

forcing the at ground-level expelled gas to be diluted in a smaller atmospheric volume. This process leads to a higher methane concentration during nighttime compared to daytime. It could partially explain the peaks found by Curiosity, as these measurements were mostly done at night time [55]. If boundary layer effects were wholly responsible for the peak observations, it would mean that the methane peak is mostly an atmospheric artefact instead of a representation of a sudden outburst of methane. However, this effect would not be able to explain the origin of the methane, given the atmospheric lifetime of methane.

Concluding: $P(life)$ can be constrained based on stellar properties. The constraint is a non-zero chance in the Bayesian framework for the emergence of life on Mars. Habitability is affected by; gravitational potential, radiation and temperature. The lower gravitational potential can mean anything from slightly altered growth kinetics to different gene expression for Earth microbes. Additionally, transport mechanisms could be kinetically different due to a different 'thin film' thickness affecting thermodynamic potentials and growth kinetics. The large amounts of ionising and UV radiation could affect microbial life at the surface. UVC would be lethal, while ionising radiation could be survived. Temperature effects can greatly influence water availability and microbial survivability. Apart from temperature-induced water shortages, the presence of water is an important factor in microbial life. These are all factors to be considered for any life form exposed to the Martian environment.

2.3. Atmospheric and surface characterisation

2.3.1. Atmospheric composition

Based on data from the Curiosity rover, the average atmospheric composition on Mars is depicted in table 2.1 [52]. A side note is the strong seasonal fluctuations observed, for example 36% for CO gas. Atmospheric pressure also experiences strong seasonal variations as shown in figure 2.2. In winter it becomes cold enough for CO_2, the main atmospheric gas, to freeze and thus be temporarily removed from the atmosphere, lowering overall pressure [52]. As can be gathered from the given atmospheric composition, the CO_2 partial pressure (between 9.0 mbar P_{CO_2} and 6.7 mbar P_{CO_2} calculated from Trainer et al. [52]) is much higher than on Earth (from 1013 mbar pressure at sea level 400 ppmv CO_2 = 0.4 mbar P_{CO_2} on earth [14]). The general atmospheric pressure on Mars is only 8 mbar, while on Earth it is roughly 1013 mbar [52].

Table 2.1: MAA composition based on Trainer et al. [52].

Compound	Vol%
CO_2	95.31%
N_2	2.59%
Ar	1.94%
O_2	0.16%
CO	0.06%

2.3.2. Soil composition around Gale crater region

The question of soil composition is twofold. Firstly is the soil composition homogeneous? Secondly, if not, the composition of the possible source location should be investigated. This question of the source region will be answered under the bio-signature characterisation. However, the actual location of the source is not too relevant as the data on the Martian soil composition is only available for locations where rovers have landed or where remote sensing data is available. Among these investigated locations is the Gale crater, where the methane peak was observed. If this is not the source region, it is likely relatively close, and the soil composition is not investigated via in-situ methods. The relevance of the soil composition is that this is the most likely place for the microbes to be. Liquid water would put the microbes into contact with this soil composition. The materials in the soil can act as a substrate on which the microbes can grow on, inhibitors that fully prevent growth or anything in between. Therefore, the soil composition is expected to greatly affect the microbial growth kinetics, but whether this effect is positive or negative needs to be investigated.

The soil composition is likely heterogeneous across the possible source region based on the orbital catalog of aqueous alteration for the Gale crater and its surroundings [6]. Remotely sensed the Gale crater floor contained: Olivine- and Fe/Mg phyllosilicate-bearing materials, Fe/Mg phyllosilicates (clays), Fe/Mg smectite, varying amounts of surface or groundwater and possibly feldspar-rich rocks [4]. Additionally, 600 mg/kg

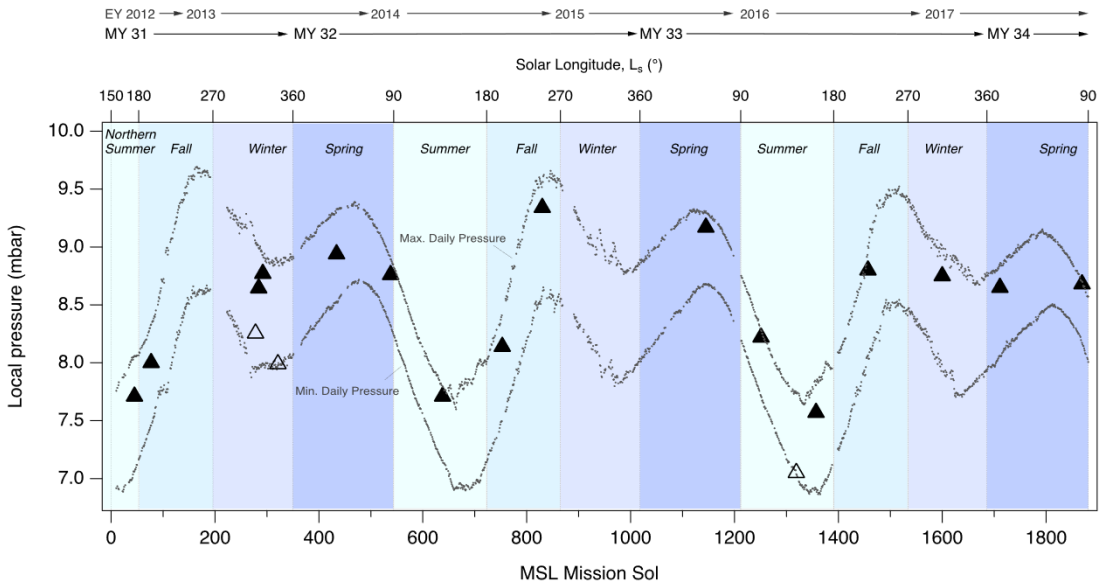

Figure 2.2: "The timing of SAM atmospheric QMS experiments is plotted as the atmospheric pressure at the time of ingestion(left axis) against the MSL mission sol (bottom axis) and solar longitude (top axis). Most atmospheric ingests for mixing ratio derivation were conducted during local night (closed symbols), with three daytime experiments (open symbols). The figure background is shaded by northern season, and the REMS daily pressure maximum and minimum values are given by the dotted lines. Seasonal trends are tracked through the direct atmospheric runs, with attention paid to possible diurnal variations. Mars year (MY) and Earth year (EY) are indicated across the top of the figure." [52]

of nitrate was found by Stern et al. [48]. Furthermore, they point to the imbalance of nitrate compared to perchlorate (>1 on Mars compared to 103 on Earth) and infer no biological activity [48]. Perchlorate was found by the SAM (Sample Analysis at Mars) unit aboard Curiosity. Lewis et al. [33] indicates that organic salts like acetate may have been present in the samples but missed in the classification step due to interference with the perchlorate and silica mesh. This possible classification error implies that acetate might be present in the aeolian deposits on the surface, enabling infiltration of these salts into deeper layers [33]. Nitrogen on Mars can be found as gaseous species with a pressure of 0.2 mbar near the surface. These nitrogen species can be transported into the subsurface via metastable thin liquid films [3]. This transport mechanism, combined with the quantity of fixed nitrogen species, allows an active nitrogen cycle [3]. While this nitrogen cycle is outside the scope of this research, it gives an upper limit of $10^{10} kg$ total biomass as a sustainable quantity [3].

According to Webster et al. [54], good regolith analogues for microbial research are P-MRA (phyllosilicate-Martian Regolith Analogue), S-MRA (sulphate martian regolith analogue) and JSC Mars-1A (low phyllosilicate regolith simulate) [54]. P-MRA especially is suitable for research in areas that have been exposed to historic pH-neutral liquid alteration, like the Gale crater [25]. The P-MRA composition as posed by Webster et al. [54] can be seen in table 2.2 and would be a good estimate for the soil composition at the Gale crater in terms of biochemical interactions and, by extension this study. Phyllosilicates are present in the Gale crater due to this ancient water-soil interaction. Thus JSC-1A is unsuitable as a simulate because of its low phyllosilicate concentration. S-MRA is equally unsuitable due to its low phyllosilicate content, as the main components in the Gale crater were identified as Fe-Mg phyllosilicates.

Summarising: the atmospheric composition will be drawn upon in the bio-signature characterisation part. The soil composition seems to be mostly phyllosilicates, with perchlorate, nitrate, and possibly acetate traces. Perchlorate levels are seen as evidence against active life, whereas nitrate levels support possible life. Acetate could also function as a substrate for different organisms. As Martian soil is unavailable, the next best thing for any research is to use an analogue. P-MRA can be used as it is similar to the composition expected in the Gale crater. Additionally, P-MRA was designed for biochemical research.

2.4. Bio-signature characterization

2.4.1. The methane peak as potential bio-signature

To further specify the methane spike as introduced in figure 1.1, the exact values are depicted in table 2.3. This study will use the values of this table 2.3 excluding the deviations as the extra uncertainty cannot be

Table 2.2: P-MRA composition according to Webster et al. [54]. This composition is a good biochemical analogue for areas like the Gale crater, which is rich in phyllosilicates.

Material	**Wt%**
Fe2O3	5
Montmorillonite	45
Chamosite	20
Kaolinite	5
Siderite	5
Hydromagnesite	5
Quartz	10
Gabbro	3
Dunite	2

quantified in combination with the high expected uncertainty from the methods that will be used. The spike seems to last at least three days before dipping down to background levels. Apart from this fast rise and fall, the atmospheric lifetime of methane on Mars is deemed too short for planetary origin or impact events to support current concentrations [10]. The lifetime of Martian methane is so short (340 years) that it can only be explained by current processes[30]. The short peaks with high concentrations require a fast process due to the six-month atmospheric mixing time [32]. If the process had been slow, the peak would have been fully mixed and thus be measurable on the entire planet as a small concentration increase. Earthly methane production must be defined to compare to the Martian methane spike. Comparing the bio-signature to the more known Earth system simplifies the search for possible life by narrowing the scope from all possible and hypothetical life to known life. While unknown life may exist, it is beneficial to first check for known life to narrow the scope of this research.

Table 2.3: Martian methane peak as described by Giuranna et al. [21]based on measurements by the Curiosity rover and planetary Fourier spectrometer.

Time [d]	CH_4 **level [ppbv]**
0	≤ 3
1	5.78 ± 2.27
2	15.5 ± 2.5
9	2.13 ± 2.02
12	≤ 5
13	≤ 5

2.4.2. Methane peak source region

The soil composition on Mars is likely heterogeneous, with oases of subsurface life, if it is present at all [30]. This heterogeneity necessitates identifying a potential source region to accurately characterise the local soil composition. The origin of the methane spike seems not to be from the Gale crater itself but a region to the east of it [21]. For this region, based on the height map in figure 2.3, the P-MRA would still be most suitable as there could have been historic water present around the indicated source areas [6]. If the squares denoted with more than 20% in figure 2.3 are assumed to be the extent of the possible source regions, then the distance between this source region and the rover sensor would be between 250 and 900 km. This distance can be used to verify potential source regions the kinetic model identifies. The denoted percentages are based on a General circulation model based on gas being expelled from a subsurface reservoir. This number is calculated by taking the proportion of simulated gas releases from a square that produces the same sensor results as were observed by Curiosity.

2.4.3. methane producing organisms living in Mars analogue conditions on Earth

Earth is a good start to investigate possible candidate species that could be responsible for the observed methane peak. Methane is produced by biotic and abiotic processes. However, biotic pathways dominate the production on Earth. The abiotic pathways are: gas, water, rock reactions like serpentinisation and magmatic processes. Thermogenic processes and methanogens represent biotic pathways [17][15]. The thermogenic

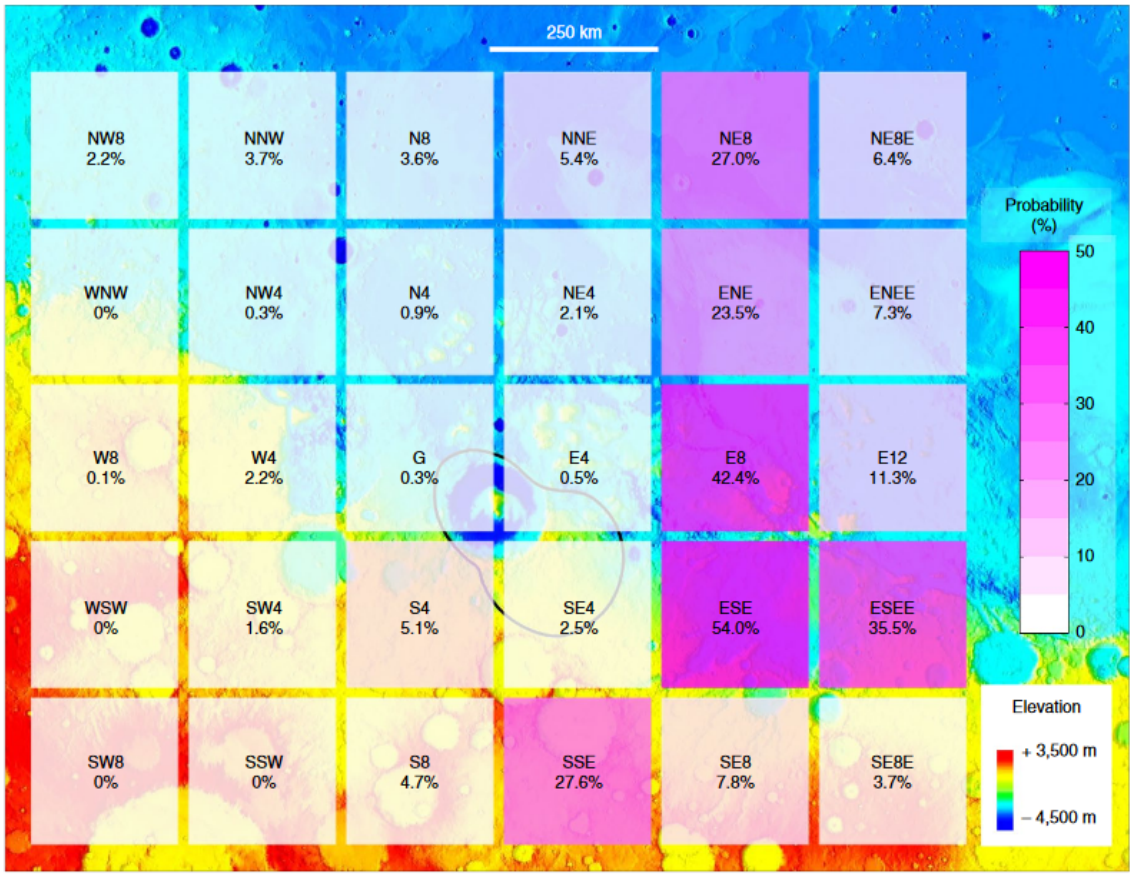

Figure 2.3: Probabilities estimated for the 30 emission sites. For each grid cell, the probability of being a source location is defined as the number of release scenarios consistent with the observations divided by the sample size [21].

processes are biological materials being transformed into natural gas due to temperature and pressure conditions. So far, no fossilised complex biological materials needed for this process have been found on Mars. The methanogens are microbes capable of digesting organic and inorganic materials, producing methane as a waste product. From these two, methanogens would be the only living ongoing process, as thermogenic processes are based on dead biological material of geologically significant age. Thus the assumption that methane was produced by methanogens is plausible. Methanogens come in three groups: hydrogenotrophs, methylotrophs and acetoclastic methanogens. Only the hydrogenotrophs can survive on an abiotic diet of hydrogen. Methylotrophs reduce methyl groups in organic molecules, and acetoclastic methanogens require a substrate of acetate, an organic salt [1]. These interactions can be quantified thermodynamically to assess the viability of the catabolic reactions. Alternatively, the catabolic reactions can be quantified kinetically to assess the microbes as chemical factories using the Monod equations for microbial growth. This kinetic quantification was done among many other models in the ADM1 model to mechanistically model the process and state of anaerobic digestors [42]. The model also calculates chemical interactions between the different states of the substrates and waste products. Methane formation by methanogens is part of this anaerobic process, making it a tool that can potentially model how methanogenesis in an anaerobic community would work on Mars. This tool will further be explored and substantiated in the rest of this chapter and chapter 3.

Methanogens in natural environments and in the ADM1 model usually aren't pure cultures. In digesters, a mixed community of methanogens, sulphate reducers, hydrolysers, acetogens, and acidogens usually occur together [39]. Sulphate present in the substrate of such a reactor is usually reduced by sulphate-reducing bacteria, in competition with methanogens for acetate, hydrogen and formate [26]. This microbial mixture produces a gas with characteristic compositions that indicate the whole anaerobic community existing. In cases where methanogens and sulphate reducers are in competition, the characteristic gas starts with a peak in hydrogen sulphide gas before methane is observed due to the difference in thermodynamic potential between the two reactions [56]. The methane peak being preceded by a hydrogen sulphide peak is a second po-

tential biosignature linked to biological methane production that could provide valuable within the Bayesian framework.

On Earth, methanogens and sulphate reducers are expected to be one of, if not the oldest, organisms based on the theory of a Last Universal Common Ancestor (LUCA) [51]. These organisms would have formed near white or black smokers and used their nutrients to metabolise [35]. These smokers are subsea vents spewing hot water enriched with minerals, hydrogen and heavy metals. The fact that these two organisms are very old and possibly the origin of life implies that they are more likely to exist on a different planet compared to more complex organisms [53]. This higher likelihood of existence allows $P(Life)$ to remain unconstrained as the number of evolutionary innovations would be very low. The chance of these organisms occurring would be close to, if not identical to $P(emerge)$ (the chance that life emerges in general). It is known that on Earth, an elevated CO_2 partial pressure has a strong effect on methanogenic activity and productivity. The elevated partial pressure of CO_2 improves activity until substrate inhibition prevents growth, thus decreasing total methane production [34]. Additionally, high partial CO_2 pressure leads to a restructuring of the microbial biome, resulting in higher methane gas concentrations [8]. These effects might also play a role on Mars, where high CO_2 partial pressures are the norm.

Based on the findings in chapter 2.3.2, Boom clay is similar to the Martian regolith. This clay type is rich in quartz and kaolinite and contains siderite [19]. The temperature of the clay layer does not exceed the Martian maximum surface temperature of 25°C. This similarity makes the Boom clay layer a potential analogue to the Martian underground, where organisms could be collected from.

Based on the above information, methanogens are the most likely candidates for biological methane formation on Mars. Assuming the existence of a mixed anaerobic ecosystem, methanogens would likely compete with sulphate reducers and be accompanied by other digestion-relevant microbes. These mixed communities of microbes could be harvested from the Boom clay, as this soil formation has mineral similarities to P-MRA. The activity and methane production would likely not be the same as on Earth due to the CO_2 partial pressure, soil composition, reduced gravity, and other factors discussed in chapter 2.2.2.

2.4.4. Thermodynamics

In order to assess the feasibility of biological activity, thermodynamic calculation of the Gibbs free energy are a useful tool [38]. Stoichiometric reactions should be defined for the microbes under investigation to assess their thermodynamic viability. Via these reactions, the Gibbs free energy can be calculated for each reaction and give an indication of the viability of the reactions on current-day Mars, provided the input concentrations are representative of that situation. To achieve representation, the soil and atmospheric composition will have to be incorporated into the Gibbs equation, together with the Martian temperature range. The exact calculation methods will be explained in Chapter 3. It should, however, be noted that the Gibbs free energy approach assumes a certain direct chemical reaction. Possible energy inputs via other microbial life or chemical equilibria changing the chemical mix are ignored. While the Gibbs analysis can provide an informed guess, it cannot definitively confirm or deny the occurrence of a reaction.

The temperature range for Mars is roughly 191K up to 294K [25]. Within this temperature range, phase changes of the medium or the individual chemical components can occur. Phase changes can have consequences for the microorganisms beyond available thermodynamic energy. As mentioned before, dormancy could help bacteria survive these cold periods, and it was found that the Martian temperature range is survivable for some methanogenic archaea. However, it is not known for the community as a whole [37]. These points are seen as enough indication that methanogens would be able to survive and produce gas to warrant further investigation. The exact steps are in Chapter 3.

Reduced gravitational potentials promote anoxic hotspots [2]. These hotspots could affect anaerobic organisms thermodynamically. However, this reduced gravity will also reduce the transport of nutrients by inhibiting convection, leaving the slower diffusion process to transport these nutrients to the cells over longer distances. This results in quicker nutrient depletion in the cell's immediate surroundings. As mentioned before, nutrient concentrations affect thermodynamic viability. Thus gravity effects can reduce growth by inducing substrate inhibition. Local nutrient depletion due to their own appetite and gas flow differing from what is conventional on Earth could lead to redox hotspots where microbes live. The effect of this local depletion will be thermodynamically investigated but not linked to quantified gravitational potentials, as this is beyond the scope of this study.

Substrate availability is a pivotal factor that affects thermodynamics and microbial viability. Available substrate steers what microbial pathways that are worth investigating. The process of radiolysis can transform pore water into hydrogen. Radiolysis occurred on Earth during the pre-Cambrian period in deep rock forma-

tions [49]. It is also speculated that radiolysis occurred during the Noachian period on Mars [49]. Hydrogen in the subsurface can act as a substrate for hydrogenotrophic methanogens, hydrogenotrophic sulphate reducers and homoacitogens. Homoacitogens could use hydrogen and carbon dioxide to produce acetate. Acetate could also be available via other unknown pathways but be missed in detection due to perchlorate/ silica interference in the detector [33]. The presence of this substrate would allow acetoclastic methanogens and acetoclastic sulphate reducers to exist. Substrate for methylotrophic methanogens is harder to identify. Organic matter containing methyl groups is part of the microbial cells, allowing the methylotrophic methanogens to live off the remains of other organisms. Based on the substrate availability and aforementioned probable inhabiting organisms, methanogenic acetoclasts, methylotrophs, and hydrogenotrophs are worth investigating, as well as sulphate reducers. As acetogens are also important to the functioning of acetoclastic methanogens, these will also be investigated based on the stoichiometry in table 2.4.

Table 2.4: The organisms, viewed as black boxes with their overall stoichiometric catabolic reactions, will be thermodynamically investigated.

Organism	**Reaction**
Hydrogenotrophic methanogenesis	$4.0 * H_{2(g)} + CO_{2(g)} --> CH_{4(g)} + 2.0 * H_2O_{(l)}$
Formate based methylotrophic methanogenesis	$4 * HCO^-_{2(aq)} + 4 * H^+_{(aq)} --> CH_{4(g)} + 3 * CO_{2(g)} + 2 * H_2O_{(l)}$
Hydrogen based methylotrophic methanogenesis	$CH_3OH_{(l)} + H_{2(g)} --> CH_{4(g)} + H_2O_{(l)}$
Methylotrophic methanogenesis	$4 * CH_3OH_{(l)} --> CO_{2(g)} + 3 * CH_{4(g)} + 2 * H_2O_{(l)}$
Acetoclastic methanogenesis	$CH_3COOH_{(l)} --> CO_{2(g)} + CH_{4(g)}$
Homoacetogenesis	$4 * CO_{2(g)} + 8 * H_{2(g)} --> 2 * CH_3COOH_{(l)}$
Formaldehyde based sulphate reduction to sulphur gas	$SO^{-2}_{4(aq)} + 2 * CH_2O_{(aq)} --> H_2S_{(g)} + 2 * HCO^-_{3(aq)}$
Hydrogenotrophic sulfate reduction	$4 * H_{2(g)} + SO^{-2}_{4(aq)} --> H_2S_{(g)} + 4 * H_2O_{(l)}$

Summarising: it is speculated that under lower gravitational potentials, the so-called 'thin film' (the interface between a cell and the bulk solution) increases in thickness, promoting anoxic hotspots [2]. Calculating the thermodynamic effects of this imbalance for several concentrations sheds light on the reaction feasibility under different equilibria. The thin film effect cannot be quantified for a given gravitational potential on Mars, but this analysis can give an indication of the evolution of the reaction. At the same time, the Gibbs free energy can also show what reactions are more likely to occur relative to the other reactions and if these reactions are feasible in the first place under Martian conditions. The reactions that will be investigated are depicted in table 2.4.

2.4.5. Kinetics

The goal of kinetic analysis of the Martian methane peak is to fill the Bayesian framework. The input of the Bayesian framework consists of three parts: P(X|life), P(X|no life) and P(life). The Bayesian framework is described in equation 2.1 and further explained in chapter 2.4.6. A visual aid is in figure 2.1. The main takeaway is that all three expressions need to be quantified to draw a conclusion on the main research question. The kinetic comparison allows the potential bio-signature to be analysed based on dynamics instead of the presence of (gaseous) compounds. This novel method could allow simpler tools to infer additional information about biosignatures. The scope of this study is biological pathways. Thus, the kinetic analysis aims to quantify P(X|life), where X in this study is the methane observation on Mars 1.1. This kinetic analysis works well depending on the applicability of the kinetic model to the Martian conditions. Therefore, the kinetic analysis should consist of two parts: firstly, an investigation into the applicability of the chosen kinetic model to Earth organisms under Martian conditions. Secondly, the correlation between the modelled gas production kinetics and the observed methane spike can be quantified.

Regarding the applicability of this kinetic model to Earth organisms under Martian conditions, the Earth organisms serve as a proxy for Mars organisms. Thermodynamic calculations provide some insight into reaction feasibility and possible nutrients being used, but they cannot be used to infer dynamic behaviour. More information is needed to assess kinetic applicability as intended in the dynamic comparison approach to the Bayesian framework. For example, the effects of P-MRA and the Martian atmosphere on anaerobic communities are unknown. Research into this has historically focused on single organisms being exposed to varying MRAs [46] [27] [28]. Most of these studies have found growth to be possible. These studies, however, did not

couple the found growth to kinetic models. The method to investigate this applicability will be outlined in chapter 3. Temperature, microgravity and radiation effects will remain outside the scope of this study but are likely large contributors to the kinetics of hypothetical Martian gas production. The reason to leave these factors out is to allow this study to reduce complexity and find the necessity for future work, in the context of the Bayesian framework method outlined by Walker et al. [53].

On Earth, anaerobic communities exist in a wide range of habitats, from swamps and tundra to the gastrointestinal tract of mammals and the deep underground, as mentioned in chapter 2.4.3. Anaerobic communities also function as valuable workers in the field of wastewater treatment. Anaerobic digesters are among the bioreactors used for anaerobic biogas production. This system being of economic and environmental importance means that much research has already gone into understanding its kinetics. Among the most impactful anaerobic digester numerical models, ADM1 is both open source, reliable and available as Python code [42] [43]. This proven model as Python code allows modifications, such as adding sulphate reducers [47]. Most importantly, it allows for a Monte Carlo analysis of the initial conditions of this system. This code will be further described in chapter 3, together with how it will practically help define $P(CH_4|life)$.

2.4.6. Bayesian inference

In order to find an answer to the first half of the main research question, a Bayesian framework as proposed by Walker et al. [53] will be used. The main question is: "how likely in percentages is the methane peak detected in the Martian Gale crater (around sol 305) attributable to a form of Earth-like life, and what form that would likely be". The first half can be answered by a Bayesian framework by finding how similar the peak is to biological activity and finding a correlation for how similar it is to systems devoid of life. With these two factors, a percentage can be calculated for how likely the observation is to occur in a system with life.

The Bayesian framework uses the Bayesian equation in 2.1 [53]. It consists of three main statistical variables and an outcome: $P(X|Life)$, $P(X|noLife)$ and $P(Life)$, where X is an observation, leading to the outcome: $P(Life|X)$. In words, these are: the chance of observing X given life is present, the chance of observing X given no life is present and lastly, the chance that life is present. This results in the conclusion the chance that life is present given X was observed. Walker further elaborates on these variables by making them conditional, $P(X|Life, C_i)$, where C_i is a condition like the presence of liquid water or carbon monoxide. As mentioned before, life in the context of this study is an anaerobic community. H_2S production in such a community could be a valuable contextual parameter based on the competition between the methanogens and sulfide reducers.

The Bayesian approach is central for estimating a conclusion and a stepping stone for broader future research into gaseous bio-signatures on rocky Earth-like planets. This future research is easily incorporated because the Bayesian framework allows new conditions 'C_i' to be added to the equation, improving the accuracy of the results.

$$P(life|X) = \sum_i \frac{P(X|life, C_i)P(life, C_i)}{P(X|life, C_i)P(life, C_i) + P(X|nolife, C_i)(1 - P(life, C_i))} \tag{2.1}$$

3

Methods

In this chapter, the findings from chapter 2 will be used to formulate methods to address the encountered knowledge gaps. The main research question is a quantified probability of the Martian methane spike being generated by life. The Bayesian framework approach will be used to reach a conclusion to the aforementioned main research question (equation: 2.1). The investigation will consist of four parts, structured so that every step increases confidence in the conclusion. These parts reduce uncertainty in the outcome by progressively increasing the understanding of the active community under simulated Martian conditions. The research topics are: Thermodynamic feasibility of catabolic reactions, the applicability of the kinetic model using experiments as a true positive, Kinetic model correlation to Martian observations, and lastly, Constructing a Bayesian framework.

3.1. Thermodynamic feasibility of catabolic reactions

An analysis of the thermodynamics of anaerobic pathways will be conducted using the Gibbs free energy code in Appendix A. This is done to dismiss the biological hypothesis early on. The magnitude of the Gibbs free energy of a pathway indicates the pathway's feasibility. If the resulting Gibbs free energy number is positive, it could be concluded that the pathway will not function on Mars. Inversely, if the number is negative, the pathway is more feasible. The investigation will be based on the thermodynamic formulas 3.1 and 3.2 to find the Gibbs free energy, combined with a database of chemicals linked to their energies at the expected Martian concentrations [12]. In formula 3.3, it can be seen that the final Gibbs energy for a fixed concentration and pressure can be expressed as linearly dependent on temperature. This property is used to simplify making diagrams over a temperature range. The factors in 3.3 are: $\Delta G^1_{T,P}$, for the Gibbs free energy corrected for concentration and temperature, R as the gas constant, z is the total number of chemicals in the stoichiometric equation, c_i is the concentration in Mol/L or partial pressure of the 'i'-th stoichiometric member, n_i is the stoichiometric factor of the 'i'-th member (positive for production, negative for consumption), $\Delta G^0_{T_s}$ is the Gibbs free energy under standard conditions, $\Delta H^0_{T_s}$ is the enthalpy under standard conditions, T_s is the standard temperature, T_x is the temperature of interest.

$$\Delta G^0_{T_x} = \Delta G^0 * \frac{T_x}{T_s} + \Delta H^0 * \frac{T_s - T_x}{T_s} \tag{3.1}$$

$$\Delta G^1_{T_x} = \Delta G^0_{T_x} + T_x * R * \sum_{i=0}^{z} c_i * n_i \tag{3.2}$$

$$\Delta G^1_{T,P} = (R * \sum_{i=0}^{z} (c_i * n_i) + \frac{\Delta G^0_{T_s} - \Delta H^0_{T_s}}{T_s}) * T_x + \Delta H^0_{T_s} \tag{3.3}$$

The initial solution for calculation will be based on the P-MRA in a watery solution under a martian atmosphere. The units are partial pressure and grams per litre. The exact values are depicted in table 3.1. The materials not in this list will get a value of 1 in the calculation. The reduction of a substrate under reduced gravity will be illustrated by reducing the first compound of the stoichiometric reaction to either 100%, 80%, 60%, 40% or 20% of the initial concentration. According to the stoichiometric equation, the other elements

are reduced or increased in the same manner. The reactions that will be investigated are depicted in table 2.4. The results of the calculations are diagrams depicting the Gibbs free energy of the different biological reactions over a temperature range. This output for the initial condition (100% of the initial concentrations) is plotted on the same graph to gain insight into the most favourable reactions and how this responds to the temperature conditions.

The calculations are performed by a Python code, optimised for easy input and output. The code can be found in Appendix A under "Thermodynamic code". The class input is the bulk solution as depicted in table 3.1, and the reactions as depicted in table 2.4.

Table 3.1: Bulk solution of watery P-MRA as was used for thermodynamic calculations.

Compound	g/L or partial P
CO2(g)	0.951
N2(g)	0.0259
Ar(g)	0.0194
O2(g)	0.0016
CO(g)	0.0006
H2(g)	1e-7
CH4(g)	1e-7
H2O(l)	1000
SiO2	3.00018
MgSiO4	2.000123084
FeSiO4	4.61892831
Fe2O3	4.61892831
(Na,Ca)0.33(Al,Mg)2(Si4O10)(OH)2·nH2O	45.0027694
Al2Si2O5(OH)4	6.366917234
FeCO3	11.14475363
Mg5(CO3)4(OH)2*4H2O	5.000307711
NO3-	0.060003693
C2H3O2-	1.600098468

3.2. Applicability of the kinetic model using experiments as true positive

Before a kinetic similarity can be drawn between modelled and observed data, the applicability of the kinetic model on the Martian condition has to be investigated. This similarity will be found by performing an experiment using organisms that live in conditions similar to Mars. The results of this experiment inform the applicability of the kinetic model. The system will run as a batch reaction based on the Martian condition where presumably very little organics are provided by aeolian transport. This transport, on the timescale of this experiment, is seen as negligible.

3.2.1. Experimental setup

Only the MRA and MAA effects will be investigated for the simplicity and feasibility of the experimental setup. The other factors described in the previous chapter will undoubtedly impact the system's kinetics. However, including them in this study would complicate the experiment so much that analysis of the results would become nearly impossible.

The MRA and MAA effects will be investigated individually and combined as shown in figure 3.1. The experimental operations are depicted in figure 3.2. For these tests, 180 ml flasks with crimp-on stoppers are used. As feed liquid, acetate and sucrose were chosen based on DSMZ 141c with the alteration to DSM2831 [20]. This feed solution was used based on the organisms known to be in the inoculum and the feed regime used by SCK-CEN, who supplied the inoculum. In these flasks, either MRA or the feed liquid is added, and a blank and control flask are prepared so that the total liquid volume becomes 100 ml, following figure 3.1. The goal is to reach a COD concentration of 3.2 g/L, the same concentration as in the P-MRA based on the chemical components. The bottles will be topped up with demi water to reach 100 ml liquid volume. Afterwards, the bottles are flushed with nitrogen gas or MAA for 5 minutes by bubbling below the surface. After closing the flasks, 20 ml anaerobic inoculum (0.18 g/L VSS) is injected, and the gas pressure is measured.

The goal is to gain data on the impact of MRA, MAA and the combination of these, compared to the blank

and fed Earth environment samples. All of these tests will be conducted in triplicate. The composition of the inoculum, MRA and MAA will be elaborated on in sections3.2.2, 3.2.3 and 3.2.4, respectively. The experiment will last eight days, with twice daily pressure measurements. At the end of the experiment, gas analysis via gas chromatography and indirect spectral absorption for H_2S gas will be performed. The 1 mL gas samples are directly fed into the GC machine after they are drawn with a glass syringe from the reactor flask. The theory for measuring sulphur gas is based on the methylene blue optical extinction method, following an internal document from the Biothane group (protocol in appendix D). The gas volume is 10mL because of the low expected concentrations. At the end of the experiment, the biomass growth is measured via VSS and TSS analysis from liquid samples taken from the unopened flasks. The gas composition and biomass growth will be compared to kinetic model results under the same 'experimental' conditions. This assessment provides an estimate of the applicability of the kinetic model to simulated Martian conditions. The kinetic model results will be generated via the method described in paragraph 3.3. In short, a triplicate via a Monte Carlo approach is conducted. The inputs are the same eight days simulation time, average initial concentration of VSS and standard deviation as measured in the experiment. The concentrations of the initial conditions are kept the same relative to each other and are universally scaled to get the initial VSS the same as the experiment.

Test A1		**Test A2**	
Water	100 mL	Water	83 mL
Culture	3.6 mg VSS	Culture	3.6 mg VSS
MRA	20 g	Feed	17 mL
N2 flush	5m	MAA flush	5m
		Test B1	
		Water	100 mL
		Culture	3.6 mg VSS
		MRA	20 g
		MAA flush	5m
Blank		**Control**	
Water	83 mL	Water	100 mL
Culture	3.6 mg VSS	Culture	3.6 mg VSS
Feed	17 mL	N2 flush	5m
N2 flush	5m		

Figure 3.1: A table depicting all experiments conducted, with contents of the flasks. This experiment is conducted to assess the effects of MRA and MAA on gas production and biomass growth of a cultured natural anaerobic community.

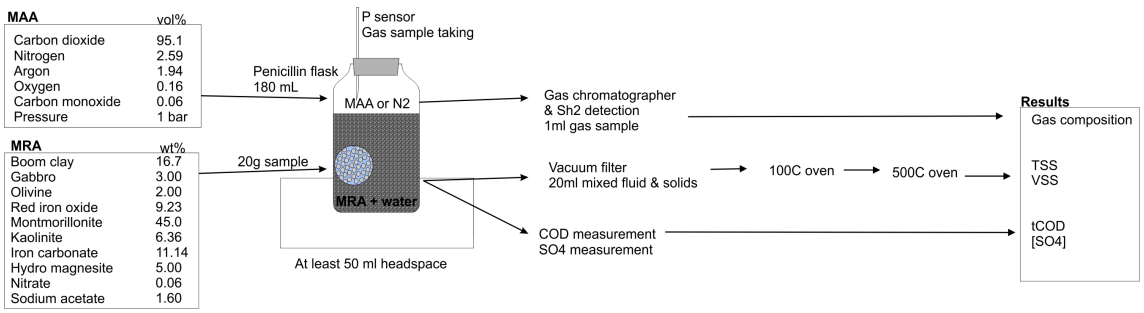

Figure 3.2: Flowchart depicting the experimental setup, the vessel and quantities depicted are for all experiments.

3.2.2. Mars analogue organisms

As Martian microbes have yet to be found, the next best thing is to investigate Earthly microbes and see how they respond to simulated Martian conditions. The best thing is to find an anaerobic microbial commu-

nity already adapted to Mars analogue conditions. The Boom clay layer has strong similarities to the P-MRA mineral composition [19]. The microbes living in the pore water are thus adapted to the expected Martian mineral composition. The possibility of Martian microbes living under the surface due to radiation is also represented in the depth at which the boom clay microbes are sampled. SCK-CEN (Belgian nuclear research centre) operates the HADES research site at 225 meters deep. Microbes living here in the Boom clay pore-water are adapted to the Martian mineral composition and underground life. The microbes were provided in a cultured pore water solution by SCK-CEN for this study to find the effects of simulated Martian conditions on biotic gas production kinetics.

3.2.3. MRA

The MRA used is based on the P-MRA by Maus et el. [36]. However, due to supply issues, chamosite was unavailable. Additionally, quartz was replaced by the quartz fraction in 'Boom' clay, while the chamosite was replaced by increasing the fraction of hematite, siderite and kaolinite. Siderite was replaced by red iron pigment, which was reported to be pure Fe_2O_3 by the vendor. Gabbro and olivine were won from rock samples. Additionally, nitrate and acetate were added based on the research by respectively Stern et al., and Lewis et al. [48][33]. Thus, the overall MRA composition is made by weight percentage, as is depicted in table 3.2. Acetate was added even though its presence on Mars has not definitively been confirmed to give this hypothesis of life on Mars an optimistic chance of succeeding. It will be a definitive result if life is unlikely under these favourable conditions. When life under these conditions proves likely, further research under stricter conditions is needed.

Table 3.2: P-MRA composition based on Maus et al. with changes due to availability of materials [36].

Compound	**wt%**
Gabbro	3.00
Olivine	2.00
Red iron pigment	9.23
Montmorillonite	44.97
Kaolinite	6.36
Siderite	11.14
Hydromagnesite	5.00
Nitrate	0.06
Acetate	1.60
Boom clay	16.65

3.2.4. MAA

The composition of the MAA is based on the average Martian atmosphere as described in table 2.1 [52]. Hydration will be a consequence of the test, not a controlled variable. The pressure at the start of the experiment was slightly above atmospheric to reduce air ingress and was thereafter closely monitored. The average composition of this gas is used to find its effects on gas production.

3.3. Kinetic model correlation to Martian observations

The kinetic comparison uses three code blocks that, together with their data flow, are depicted in figure 3.3. The three blocks are: the ADM1 class, the dilution algorithm and the Monte Carlo (MC) analysis algorithm. The ADM1 class block describes all kinetics. The dilution algorithm serves to couple the kinetics black box to the observations. The MC algorithm analyses the results of this system compared to the observations. The actual code of this method can be found in the "ADM1 Monte Carlo code" in Appendix A.

3.3.1. ADM1

The used ADM1 model python implementation is intended for modelling anaerobic bioreactors using high organic loads [43]. Thus it is not ideal to model the situation on a different planet in scarce nutrient conditions. However, given the bounds of this study, it is the most flexible software model that comes closest to Earth-based reality. The simulation of the microbial community will be done based on the available MRA, MAA compositions and the ADM1 code by Sadrimajd et al. [43]. The ADM1 code is extended by hydrogenotrophic sulphate reducing bacteria (hSRB) simulated according to Solon et al. [47]. This combined

code will only be altered to make it more legible but will not be changed functionally. Legibility and run-time improvements were achieved using a vector approach to the concentration variables, allowing the separate algorithms to exchange their states more easily. Additionally, the data was put into a data frame once the simulation was done completely, significantly reducing processing time. Restructuring the code into a class-based architecture allows external code to use the ADM1 model more simply as a black box.

3.3.2. Dilution

The dilution algorithm calculated a theoretical distance and time shift between the modelled data and the Martian methane peak. The assumption of the Mars rover measuring gas directly above a vent is very unlikely, necessitating this dilution approach. The dilution algorithm will pick the maximum value of the Mars methane data and the maximum of the simulated methane data. It will then use these two data points to calculate the distance between the virtual vent (assumed to be a gas point source) and the Rover measurement inlet. This distance is based on the digital reactor's gas volume being diluted in half a sphere with a radius 'r'. Here, 'r' is the distance between the point source and the detection point. This concept is illustrated in figure 3.4. The maximum of the observation is not likely to be the actual peak concentration of the observed event based on measuring frequency. However, this method works better than not performing it.

The Martian data can also be shifted in time, as the simulated data is mathematically time-invariant. Based on the maximum concentration occurrence, the two systems can exist in a unified time frame by ensuring the two points of maximum concentration occur simultaneously and no part of the data exists before t=0. This method avoids a low correlation due to different starting times rather than a lack of similarity and errors due to Python mishandling negative time. The time shift will be unable to find a starting time for the Martian data. However, using the peak as a fixed point will give more accurate statistical estimations than not shifting in time.

3.3.3. Monte Carlo and statistics

Monte Carlo analysis allows for assessing the impact of the initial reactor and concentration conditions on the gas kinetics. A Pearson correlation is used to assess the similarity between the observation and the simulations as it is agnostic to magnitude differences and focuses on the rate of change similarity. This method ensures that no data points have to be sacrificed for magnitude correction like the dilution method. Doing this reduces the uncertainty of the Pearson correlation between the Martian data and the modelled data due to uncertainty in the initial conditions. The initial conditions are the substrate and biomass concentrations and the reactor liquid and gas sizes. The average values for these are the same as in the initial code, apart from the newly added concentrations and the changed variables in table 3.3. All initial conditions are assigned a 33% standard deviation, as this is the highest possible deviation before the normally distributed variables can sometimes reach negative values crashing the simulation. To properly use the MC approach, the initial conditions are set 2500 times in the same amount of simulation. A single simulation will last 18 simulated days to capture enough time to time shift the data. The model is set up as a batch reactor by reducing the inflow to 0.

Table 3.3: Changes and initial values in the initial conditions of the ADM1 model as it is used in the MC analysis. S_IS, S_SO4, X_hSRB, S_H2S and S_gas_H2S were newly added as sulphate reducers were not initially in the model.

Initial condition	Initial model value	Used value	Difference
S_ac	8.93E-02	1.35E+00	1.26E+00
S_h2	2.51E-07	1.00E-05	9.75E-06
S_ch4	5.55E-02	0	-5.55E-02
S_co2	9.47E-03	7.61E-03	-1.86E-03
S_gas_h2	1.10E-05	1.00E-05	-1.00E-06
S_gas_ch4	1.65E+00	0	-1.65E+00
S_gas_co2	1.35E-02	7.61E-03	-5.93E-03
S_hco3_ion	8.57E-02	8.57E-04	-8.48E-02
S_IS	0	2.51E-07	2.51E-07
S_SO4	0	1.24E-02	1.24E-02
X_hSRB	0	6.77E-01	6.77E-01
S_H2S	0	0	0
S_gas_H2S	0	0	0

The Pearson correlation was calculated over the non-diluted gas dynamics to avoid sacrificing data points where it was not needed. This test shows the statistical likely hood the two data sets are unrelated (null hypothesis). The time shift was, however, still applied to the modelled data for comparison. This correlation provides an input value for the Bayesian model. A positive correlation is assumed for a correlation derived from two-tailed p-values below 0.01. The proportion of simulations where this is the case compared to the total number of simulations will be $P(CH_4|life)$.

Apart from the MC approach, a linear regression between the two data sets can be constructed. The regression only illustrates how well the Martian methane peak and diluted data correlate. Quantification can be achieved by calculating the root mean square error (RMSE) between the data points and the 1-1 line. The combination of regression and dilution also visualises the method behind Pearson's correlation coefficient on a single example instead of different random samples. Doing this lacks the mathematical rigour of the MC method but provides a more intuitively understandable image.

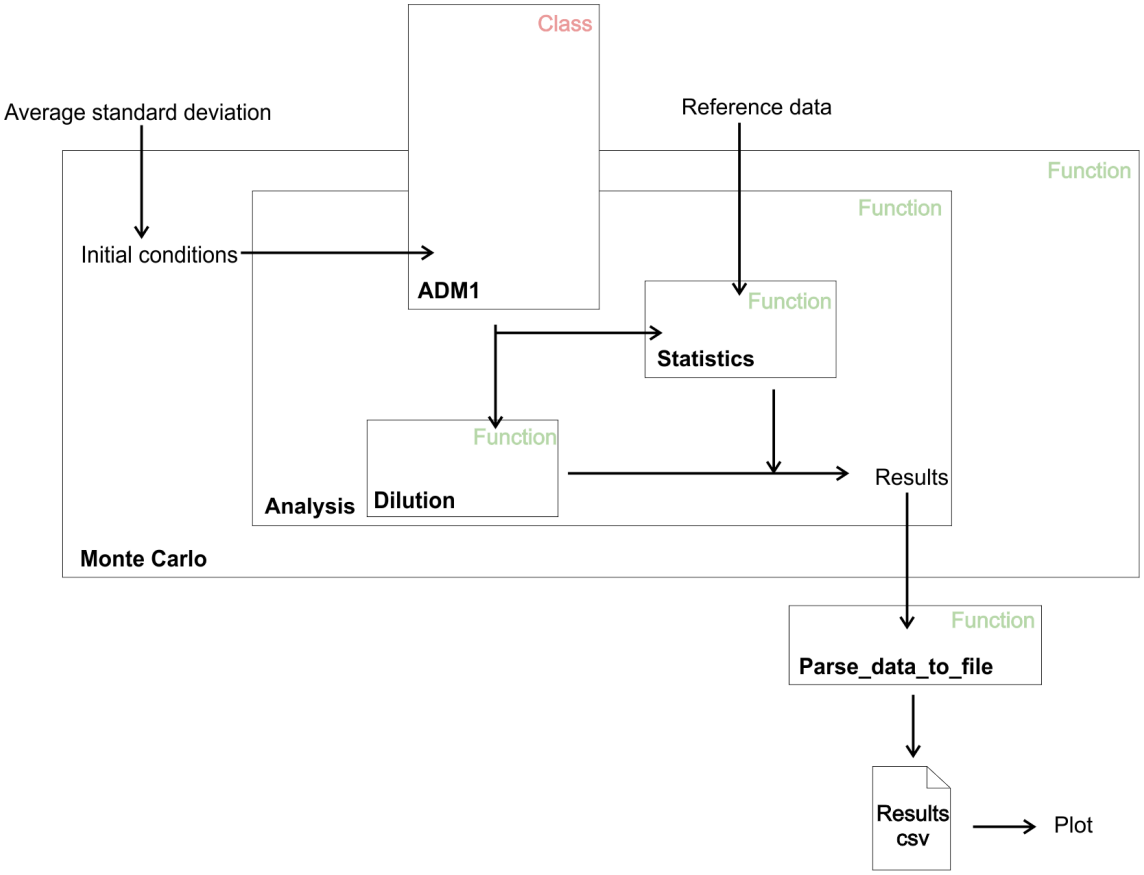

Figure 3.3: Flowchart depicting the code architecture for the Monte Carlo analysis of the ADM1 model compared to the Martian data. The three code blocks depicted are: ADM1 class, dilution function and Monte Carlo function. The boxes depict the reach of the local variables within the python code. The Monte Carlo function uses the analysis function to simultaneously calculate the outcomes from the dilution function and the statistics function that generated the correlation values. The ADM1 class is independently callable but, in this case, is called within the analysis function. The data is depicted as text without blocks, where the arrows depict the flow. The initial conditions are edited within the Monte Carlo function based on the average standard deviation. This last is defined as an independent input. These varied initial conditions are passed to the ADM1 class to generate dynamic model outputs. The dynamic output of the ADM1 model is used together with "Reference data", which is also an independent input. These two data streams are used in parallel to find the dilution factor and correlation to the Martian observation. Within the analysis function, this is bundled into a results dataframe. After the MC function has finished all its simulations, the "Results" data is parsed to a last function that writes the results to a 'CSV' file. From this file, plots can be made.

3.4. Constructing a Bayesian framework

The Bayesian formula will take the proportion of model outputs with correlation $p-value < 0.01$ as $P(CH_4|life)$. A range between 0.1 and 0.9 for non-biological correlation $P(CH_4|nolife)$ will be used, as no exact numbers were found in literature. Apart from being known as non-zero, $P(life)$ could not be constrained and will

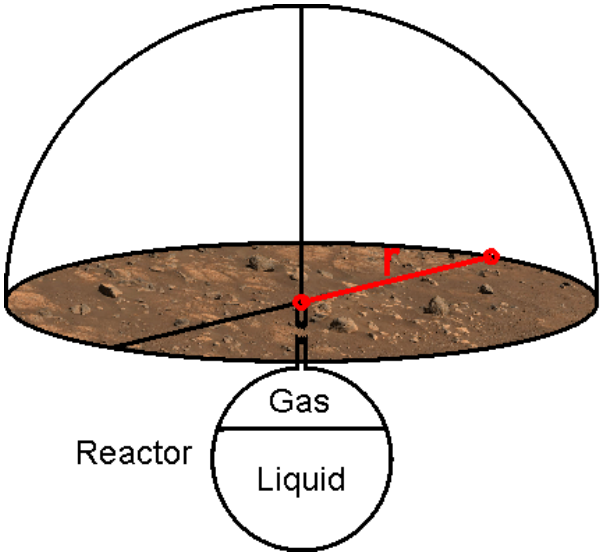

Figure 3.4: Dilution calculation illustration. The dilution of the reactor gas volume in the volume of a half dome with radius 'r', where 'r' is the distance between a theoretical point source and the sensor ingestion point denoted by the red line marked with 'r' in this graph.

range between 0.1 and 0.9. This exact variable range was chosen as the chances 0 and 1 only provide trivial results, while the range still covers the largest part of the probability space. The outcome will be a plot indicating $P(life|CH_4)$, producing a graph indicating chance based on other chances.

4

Results

In this chapter, the results for the methods proposed in chapter 3 are given, reusing the same research topics structure. The research topics were: "Thermodynamic feasibility of catabolic reactions". Here the Gibbs free energy of different metabolic reactions from the anaerobic community was calculated. This gave insight into what reactions are thermodynamically favourable under Martian conditions. The potential effects of microgravity are also touched upon. Secondly, for "Applicability of the kinetic model using experiments as true positive", an experiment was conducted into the effects of MRA and MAA on the functioning of a microbial community. Third, for "Kinetic model correlation to Martian observations", ADM1 was used to predict the values expected in the experiment described in chapter 3.2 and on Mars. A Monte Carlo approach was used to reduce the uncertainty of outcomes caused by the uncertainty of the initial conditions. The results comprised a Pearson correlation coefficient between the modelled gas and the observed methane peak and a theoretical distance between the microbial community and the rover. A linear regression analysis was also conducted to find the correlation visually. Lastly, for "Constructing a Bayesian framework", the kinetic results were used in the Bayesian framework to quantify the likelihood of an anaerobic community being responsible for the measured methane on Mars.

4.1. Thermodynamic feasibility of catabolic reactions

The Gibbs free energy potential of a reaction dictates the likelihood of that reaction occurring on Mars. The likelihood of this in a community with other microbes can be found in their respective Gibbs potentials. Deceptively, negative energy is more energy available for the microbe during a reaction. Gibbs free energy magnitude can also indicate the succession of multiple reactions in a mixed bulk solution.

Under Mars conditions, the Gibbs free energy for the stoichiometric reactions listed in table 2.4 have been plotted in figure 4.1 on the Martian temperature range. It can be seen that a sulphate reduction reaction has the lowest Gibbs energy, making it thermodynamically advantageous for organisms performing this reaction before 'downgrading' to acetoclastic and methylotrophic methanogenic reactions. This hierarchy can indicate the order in which gasses can be observed. The other analysed reactions occur much closer to equilibrium. Homoacetogenesis is thermodynamically unlikely to occur at all.

The results of the microgravity-affected single pathway calculations are depicted in figure C.1 and C.2 in appendix C. The exact values of these plots can be found in appendix B. In short, the simulated microgravity only has significant effects on reactions close to the thermodynamic limits. Homoacetogenesis remains thermodynamically unfavourable under the Martian temperature regime. On the other hand formate based methylotrophic methanogenesis, Hydrogen based methylotrophic methanogenesis, methylotrophic methanogenesis, acetoclastic methanogenesis and formaldehyde-based sulphate reduction will likely occur under the Martian temperature regime. Only hydrogenotrophic methanogenesis and hydrogenotrophic sulphate reduction are in between cases. Depending on temperature and concentration, these reactions produce enough energy to survive.

4.2. Applicability of the kinetic model using experiments as true positive

An experiment was conducted to investigate the difference in gas and biomass production of an anaerobic microbial community due to Martian conditions, as outlined in chapter 3. The biomass growth between the

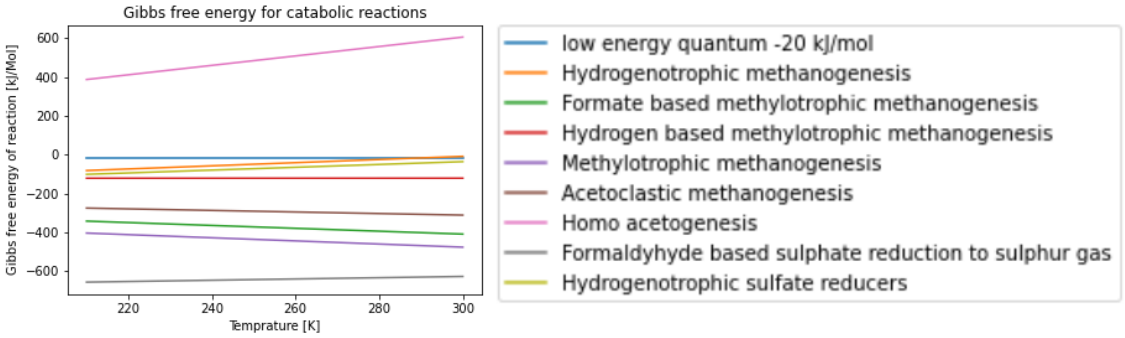

Figure 4.1: Under conditions defined in table 3.1 and Appendix B, the Gibbs free energy of all reactions from table 2.4. The most likely being formaldehyde-based sulphate reduction. Methanogens of all three types are likely after this. The x-axis contains the temperature on Mars in Kelvin. The Gibbs free energy on the y-axis is plotted for all reactions in the legend regardless of phase changes of the reagents and medium.

start and end of the experiment can be gathered from figure 4.2a. The experiment produced more biomass than the ADM1 model predicts.

In terms of methane content in the gas phase, all experiments were within one standard deviation of each other, as can be seen in figure 4.2b. However, the same does not go for hydrogen sulphide production. The ADM1 module underestimates this production by three orders of magnitude.

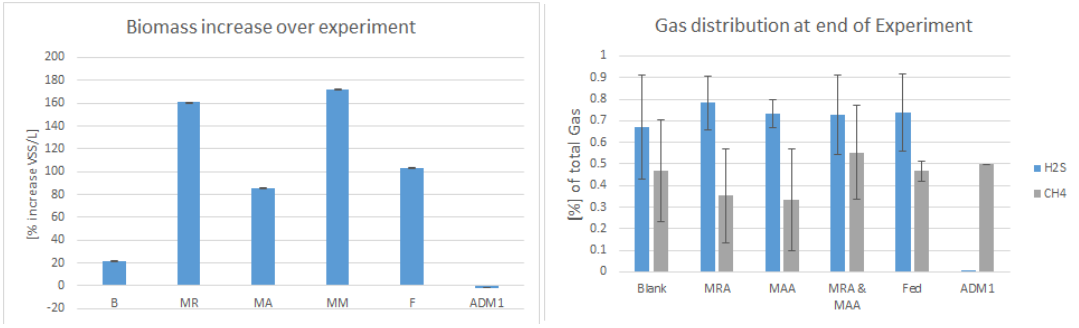

(a) (b)

Figure 4.2: Experimental data gathered according to the methods outlined in figure 3.2. 4.2a: The average total biomass growth for the experiment. Both MRA samples show excess growth, while the ADM1 model predicted a very small decrease in biomass. 4.2b: The average CH_4 and H_2S content in the gas phase at the end of experiments for the experimental conditions and the ADM1 model.

4.3. Kinetic model correlation to Martian observations

The ADM1 python model was combined with the equations from Solon et al. [47]. The initial results of this simulation are visible in figure 4.3 and represent a single integration in the MC analysis. The correlation was calculated from the non-scaled data in figure 4.3a, whereas distance was derived from the dilution algorithm output visible in figure 4.3b. As the effect of the initial conditions was unknown, the Monte Carlo simulation in figure 4.4 was used for the results in table 4.1. It is interesting to note that in terms of biology, hydrogenotrophic organisms dominated the biome for the first two days, as seen in figure 4.3c. The peak of hydrogenothrophs coincides with the simulated methane peak in time.

With a p-value of at least 0.01 (10.0e-3), the null hypothesis of coincidental correlation can be rejected in 77.9% of the cases. The average p-value gained from the MC procedure was: 9.45e-3 +/- 1.22e-3 as seen in table 4.1 and figure 4.4a. The distance distribution in figure 4.4b shows a skewed, normally distributed shape, similar to the p-value. The distance is centred around 5 km.

After the simulation has been' diluted', the linear regression approach between the simulation and observed data can be seen in figure 4.5a plotted in the time domain. In figure 4.5b, the data matches very well with the 1-1 line, indicating a strong similarity between the observations and simulation. This is distinctly not true for figure 4.5c.

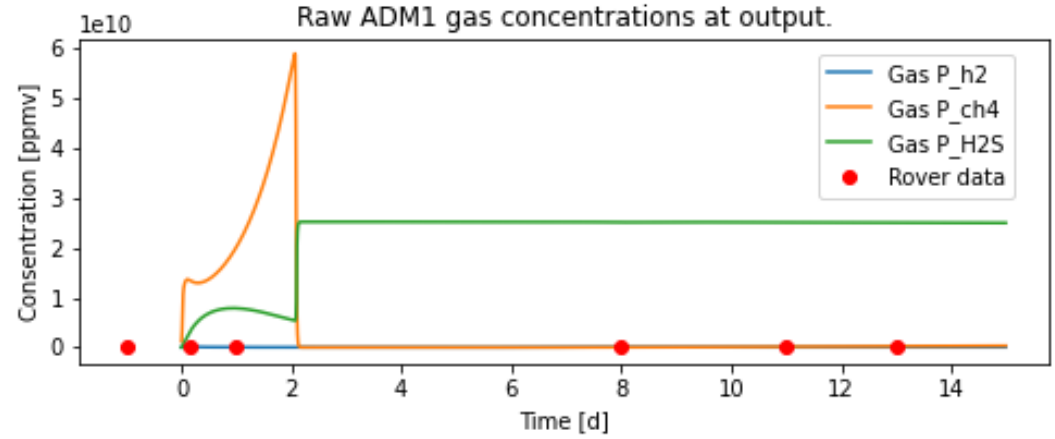

(a)

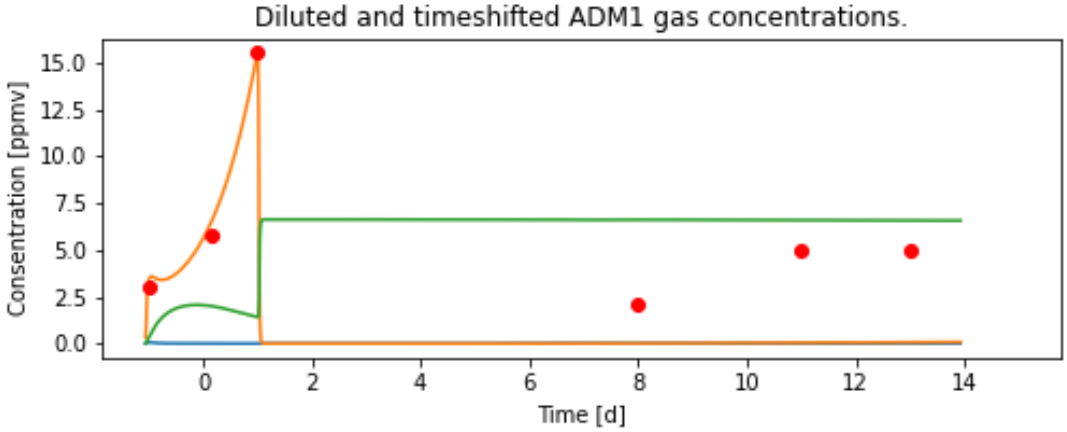

(b)

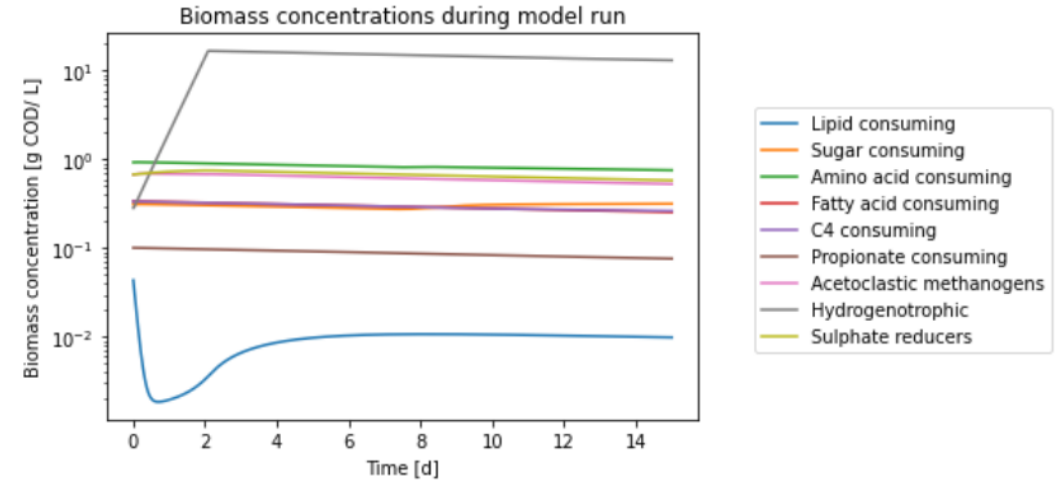

(c)

Figure 4.3: 4.3a: The gasses are expelled at a theoretical point source between the 'reaction vessel' and the Martian atmosphere. The composition is based on the ADM1 model outputs. 4.3b: Outputs of the ADM1 model, combined with a basic dilution of the model data, and the time shift of the Mars data [21]. Based on a half dome of the designated radius, causing dilution of the concentrations found in figure 4.3a. This combination shows a promising fit between the first two methane data points and the simulation. 4.3c: Biomass from the same ADM1 run as the surrounding gas production plot on a log axis. Hydrogen-consuming organisms show strong growth on the first two days, while lipid-consuming organisms decay in that time frame and rebound when the hydrogenotrophic feast is over.

.

Table 4.1: Monte Carlo generated values representing the four main components of the fit between the Martian methane spike and the kinetic model. The maximum, minimum, average and standard deviation of the correlation-based p-value and the calculated distance between source and sensor.

	P-value	**Distance [m]**
Maximum	0.018	6590
Minimum	0.008	3110
Average	0.009	5090
Standard deviation	0.005	470

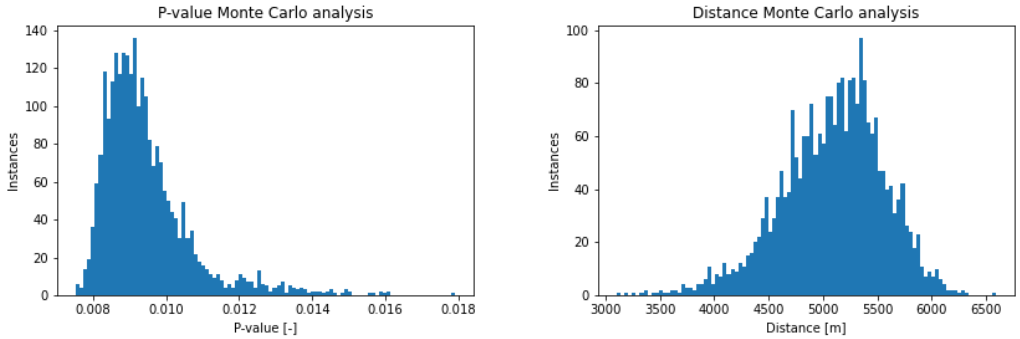

(a) (b)

Figure 4.4: The results from the Monte Carlo analysis showed skewed normal distributions. 4.4a: The two-tailed p-value based on the Pearson correlation coefficient. $p < 0.01$ is assumed to be a good fit, this happens in 77,9% of the simulations. 4.4b: The distribution of inferred distance based on the peak matching method is described in 3.3.2. This inferred distance is between the source and sensor, which is expected to scale the modelled data towards the in situ measurement.

.

4.4. Constructing a Bayesian framework

The results from the Bayesian analysis for methane (figure 4.6) indicate that $P(life|CH_4)$ for $P(CH_4|nolife) = 0.9$ is slightly below $P(life)$, for any input $P(life)$. However, $P(life|CH_4)$ becomes larger than the input value $P(life)$ for all values $P(CH_4|nolife) < 0.779$ at the hypothetical source.

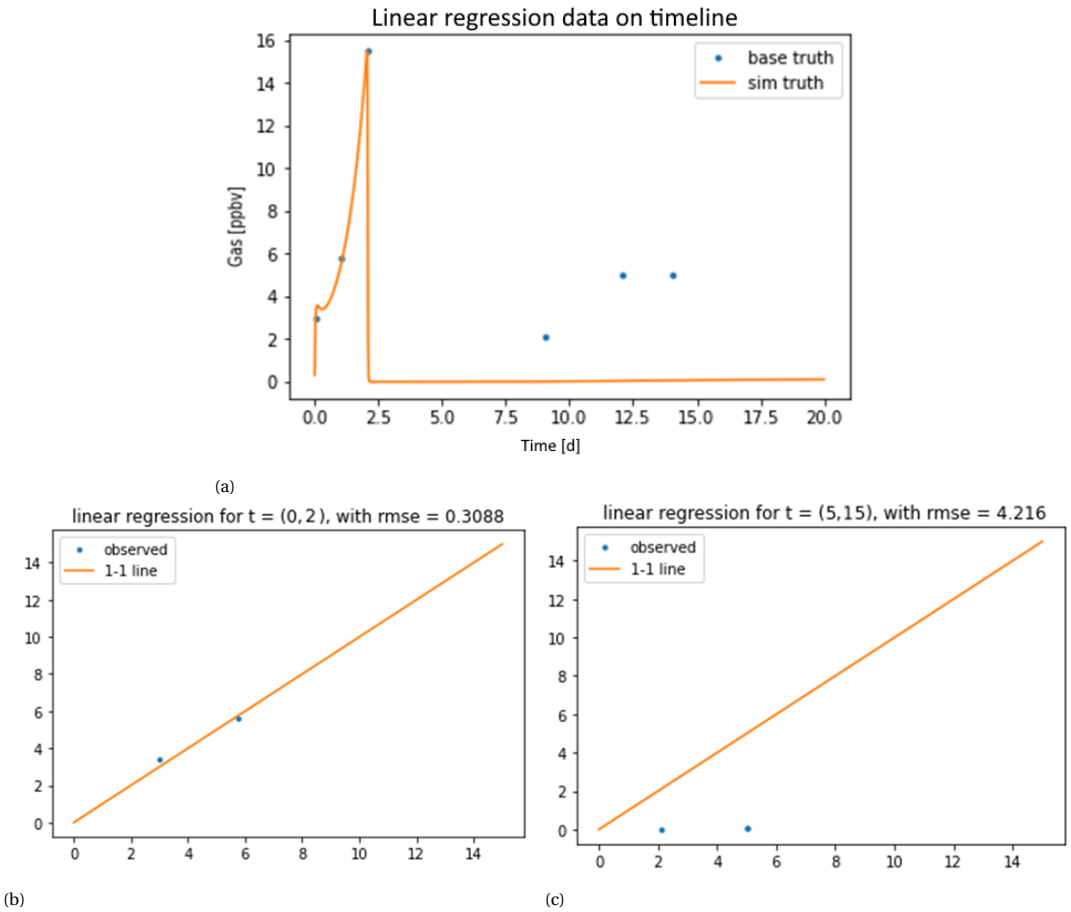

Figure 4.5: Linear regression towards a 1-1 fit of the Martian peak data compared to the model output after dilution. The y-axis is shared between all plots. 4.5a: The gasses expelled at a theoretical point source between the 'reaction vessel' and the Martian atmosphere, this data is used for the 1-1 linear regression after the dilution code has been used on it. The point at t = 2.5 [d] should be disregarded as it was used to scale the model output. 4.5b: The points between t = 0 and 5 [d] nearly lie on the 1-1 line. The RMSE being 0.30 reinforces this.

. 4.5c: The data points between t=5 and t= 15 [d] show no connection to the 1-1 line. The RMSE shows this as well with an error of 4.2, much higher than for the points between t = 0 and 5 [d].

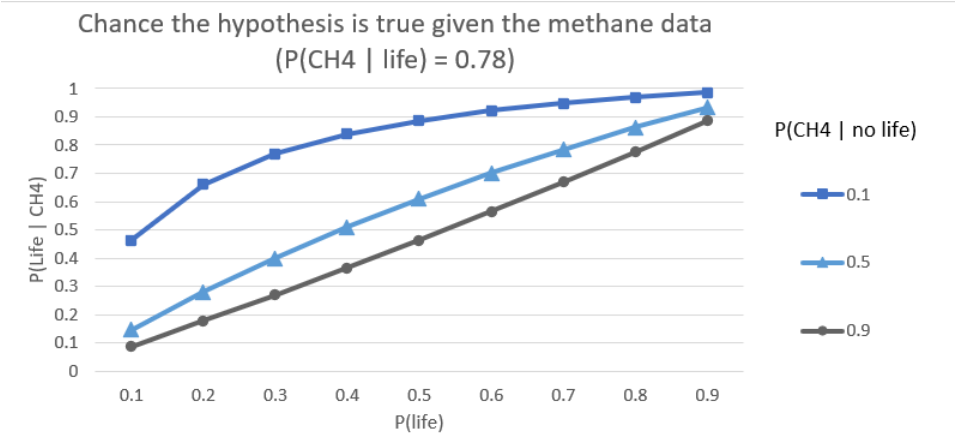

Figure 4.6: Methane-based inference of the chance life is present on Mars, based on the methane observations P(Life | CH_4). 77.9% of the simulation showed strongly correlated behaviour to the observed data ($p < 0.01$). This number is the chance that the methane peak is generated by life P(CH_4 | life). The three lines show three assumptions for P(CH_4|no life), the probability methane is being produced abiotically. The x-axis shows the 'prior' confidence in life existing near the Gale crater P(life). These three probabilities can generate a 'posterior probability' using equation 2.1 to generate the number on the y-axis. The y-axis depicts the posterior likelihood of observing life given the methane observation P(life | CH_4). The posterior lies above the 1-1 line for any given prior, assuming P(CH_4 | no life) < P(CH_4 | life). If this is not the case, the posterior lies slightly below the 1-1 life. A posterior likelihood above the prior indicates that observing a correlated methane peak is a strong indication of possible life.

5

Discussion

In this chapter, the results presented in chapter 4 will be discussed. The results are supposed to answer the research questions posed in chapter 2 to support the conclusion to the main question. This main question is: what is the chance in percentage, that Earth-like life was responsible for the methane spike around sol 305 (13th of June 2013)? The research questions posed were dividable into four groups. These groups are the thermodynamic feasibility of catabolic reactions, the applicability of the kinetic model using experiments as true positive, kinetic model correlation to Martian observations and lastly constructing a Bayesian framework. The exact aims and discussion of results can be found in the respective sub-chapters below.

5.1. Thermodynamic feasibility of catabolic reactions

The three thermodynamic research questions were; "what catabolic reactions are thermodynamically feasible", "in what sequence will these reactions occur thermodynamically" and "what is the role of micro-gravity on this hierarchy and feasibility".

Most reactions were found to be feasible, mainly methanogenic and sulphate-reducing pathways were at the top of the hierarchy. These are most likely to occur under the approximated Martian conditions. It should be noted that a thermodynamically feasible reaction does not guarantee that a reaction will occur. On the other hand, a thermodynamically unfeasible reaction will not occur. Homoacetogenesis fell in the category of an unlikely reaction. This reaction is not present in the kinetic model. The absence is corroborated by investigating the kinetic functions of ADM1 [42]. The acetate kinetics only show biological utilisation. The kinetics for CO_2 show only biological addition and abiotic loss; only hydrogenotrophic methanogens act as hydrogen sink. The homo acetogenic pathway in the Gibbs equation affected all of these substrates. The exclusion of unlikely reactions from ADM1 is good, as this mechanistic model ignores thermodynamics in its calculations.

The estimate of sulphur gas being likely, aligns with Earth observations. In digesters containing the nutrients for both sulphate reduction and methanogenesis, sulphate reduction usually dominates [47]. While the soil matrix is only an approximation of Martian regolith, the thermodynamic findings for methane production are experimentally reinforced by Maus et al. [36] who found that methanogenesis can occur in MRA.

Secondly, not all soil matrix concentrations are known. The hydrogenotrophic methanogenesis pathway for example was deemed conditionally feasible based on the low estimation of H_2 concentrations. A better understanding of the ground conditions will reduce uncertainty about the validity of this analysis. For example, radiolysis could increase local hydrogen concentrations [49]. Besides hydrogen availability, most reactions showed no significant response to the micro-gravity simulation. Micro-gravity was reported to affect microbes significantly, making these findings unexpected [40]. The lack of these effects in the thermodynamic analysis could be due to the effects of micro-gravity mostly working on kinetics instead of thermodynamics.

The used temperature range for the calculations might seem unrealistic but, Lamarche-Gagnon et al. [31] found evidence for these biological processes in permafrost regions. Their findings indicate that the thermodynamic temperature calculations up to the freezing point of the water medium are accurate. Reid et al. [41] found activity as long as the medium was liquid, achieved via high salinity. Maus et al. [36] showed methanogenic activity, even in sub 0 °C temperatures in a similar high salinity medium.

5.2. Applicability of the kinetic model using experiments as true positive

The research question is: "what variables from the kinetic model are directly comparable to those observed in a Martian analogue experiment". This question focuses on methane concentration primarily, and secondarily on biomass and hydrogen sulfide gas. These facilitate the comparison between lab and Martian observations, such that a correlation between the Martian data and life can be made using the kinetic model.

For the temperature of 293 °K, MRA and MAA do not seem to impact methane production significantly. Other studies have also indicated methanogens to be active in water-saturated MRA samples [36] [13]. However, in terms of H_2S gas concentrations the kinetic model strays from the experimentally produced concentrations by three orders of magnitude for all cases. The model predicted a decrease in biomass production whereas only growth was measured experimentally. These findings mean that methane comparisons are reliable, but total biomass or H_2S predictions are not trustworthy with the ADM1 model. Thus the ADM model is suitable for modelling methane production on a simulated Mars, with the caveat that only soil composition and atmospheric composition were considered.

Furthermore, compared to the fed sample, the extra biomass growth in MRA-enriched tests does not match increased gas production. This mismatch can have two reasons: biological material in the MRA or biological weathering. In the first case, combustible material in the MRA influences the VSS measurements. The Boom clay contains organics, making this a likely explanation for the observed mismatch [19]. Additionally, a different balance between living and dead microbes, or a lower amount of hydrolysers in the experimental culture can also result in an accumulation of biological material. The second case implies that the microbes digest MRA materials without gas production. Soil weathering and chemolithotrophic reactions cannot be excluded as biological pathways, as multiple materials in the MRA mixture are weatherable [16]. Some weatherable materials in the MRA are: sulphides, quartz and Fe(II) / Mg phyllosilicates [16]. Biological weathering is mediated by microbes that do not directly produce gasses.

Hydrogen sulfide gas was detected in all samples above the detection limit imposed by the method in D. Contrary to expectations the blank samples have similar H_2S concentrations compared to the MRA-enriched samples. This is unexpected as the MRA samples contain more sulphur compounds and other nutrients and could thus produce more H_2S gas compared to the blank test with only inoculum in water. This lack of difference could be explained by (i) the low VSS concentration of the inoculum or (ii) a problem with the detection method. Very low sulphur reducer numbers in the inoculum could ensure that these microbes were not able to use up most of the nutrients. Thus, substrate inhibition did not influence the total gas production, even for the sample without added substrate. The nearly identical concentrations could indicate possible problems with the measurement method or used reagents. However, the ADM1 model predicted even lower sulphur gas levels. The discrepancy between the model and experiments could be explained by the model lacking both iron chemistry and SRB (Sulphate reducing bacteria) pathways. Only h-SRB (hydrogenotrophic sulphate reducing bacteria) from Solon et al. [47] were added to the ADM model. Methylotrophic, acetoclastic and propionate oxidising SRB could be included based on Solon et al. [47].

5.3. Kinetic model correlation to Martian observations

The kinetic comparison aims to find a correlation between the Martian methane observations and the model results. This correlation will be used to assess the main research question using the Bayesian framework.

It should be noted that the initial model conditions were not representative of the sparse conditions envisioned in the Martian (sub)surface, but based on the initial conditions of an anaerobic reactor as given by Sadrimajd et al.[43]. This effect was mitigated by the actual conditions being within the range of the MC simulation. However, the actual initial conditions being only a subset of the used initial conditions means that the actual outcomes are also only a subset of the outcomes. The outputs representative of the Martian conditions could be obfuscated by results that are not representative.

The distance calculation results, indicate that the dilution model is a simple yet effective tool for matching the data. Thus the connection between the source and sensor data is at least similar to, or dominated by, a scaling process like dilution. However, the found distance of 5 km as opposed to 500 km as proposed by Giuranna et al. [21] means that while this method has some validity, either it or other parts of the model are not yet accurate. Atmospheric boundary layer conditions for example could be more important than simple dilution [55].

Based on linear regression to the model, the Martian peak seems to consist of not one but two regimes. The first two data points follow the shape of biological production, while the last three follow a different trend. While low RSME (root mean square error) values show promise, these values can only be so low when one of

six data points is sacrificed in the dilution fitting process, reducing statistical significance.

The ADM1 module falls short in modelling Martian conditions because of the lack of robustly implemented temperature effects. The temperature should at least affect: chemical phase changes and microbial activity [42]. The temperature in the module is assumed to be constant during a simulation, preventing the Martian diurnal cycle to be taken into account. This cycle has been found of importance to accurately describe small-scale methane plumes on Mars by Mickol et al. [37]. Both of these temperature-related shortcomings prevent the implementation of freeze-thaw cycles and investigating their effect on the gas production. Freeze-thaw cycles could fundamentally change the correlation by introducing inactive cold periods.

While the Monte Carlo analysis reduced and quantified uncertainty in $P(CH_4|life)$, the lack of Martian data cannot be left unremarked. Even though the statistical correlation was significant, this has only been tested for a single event. Repeating this method on multiple methane peaks reduces the chance of falsely inferring a correlation that only applies to a single event.

No explicit methylotrophic methanogens are implemented in the ADM1 model. Based on the Gibbs analysis in figure 4.1, this group seems likely to be active. Similarly, only a single type of sulphate reducer was implemented, with sulphate phase equations based on Solon et al. [47]. The lack of SRBs limits detailed analysis of the separate species of gas producers and gas products. In part this sulphur problem is described in the kinetic applicability of the model. Furthermore, the ADM1 software was made with the integrated formulas by Rosen et al., preventing easy future expansion of capabilities [42]. The results from the distance calculation show another discrepancy. The found distance was around 5 kilometres, while a distance of around 500 kilometres would be more likely according to Giuranna et al. [21]. The dilution method for this distance indication assumes an unobstructed gas flow from the subsurface to the atmosphere. The dilution method oversimplifies the intricacies of subsurface transport, atmospheric transport and extinction processes, and their effect on the detectable plume. Therefore, this distance should only be seen as an indication, not a feasible localisation method. Secondarily, this distance indication is strongly affected by the initial liquid and gas volumes of the model. These are unconstrained, contrary to the biomass constrained by Boxe et al. [3] to $10^{15} kg$. This limitation is due to the nitrogen availability on Mars. However, the biomass cannot be quantified by the ADM1 model based on the kinetic applicability. There is a strong relation between biomass and distance and a strong correlation between model values and martian data. This correlation implies that dilution is fundamental to the transport process between the source and the sensor.

Lastly, the geological context of a possible community could differ from the surface composition around the Gale crater on which the P-MRA was based. Thus the presence of local (inhibiting) compounds and soil moisture conditions are uncertain. Additionally the assumption of a batch situation is unknown. From both a thermodynamic and a kinetic perspective the assumption of a batch reactor without substrate input, can be deemed unlikely. Kinetically, in a batch system the microbes would be prone to extinction due to the substrate being reduced to gas and lost to the microbial community. If extinction has been going on for geological periods, the Martian observation of a current biological gas expulsion would be highly unlikely. However, the possibility of a slow substrate influx on a longer timescale compared to growth could support an ecosystem with long dormant periods.

5.4. Constructing a Bayesian framework

The Bayesian framework was used to infer $P(life|CH_4)$ from the found correlation P(CH_4|life). The two questions that are answered with this statistical method are: firstly, what is the probability $P(life|CH_4)$ and secondly, "is the combination with H_2S a valuable bio-signature combination". The answers to both questions can be found in chapter 6. Although it is possible to quantify $P(life|CH_4)$, the outcome is not entirely true to nature.

The Bayesian formula is wholly dependent on its inputs meaning that the effects between biological gas production and detection, which affect the rover data but do not effect the modelled data, would change the Bayesian results. Therefore, finding representative values for the correlation is very important to the accuracy of the Bayesian results. Even with the kinetic model being improved to perfection, experimental corroboration of the results would still be missing. Before this experimental proof of the kinetic model has been gathered, and more data points from Mars have been compared, the Bayesian values will be no more than initial estimates. Estimates that can easily be improved by future work using the Bayesian framework. This easy improvement is due to the nature of the Bayes equation as a formula for changing beliefs in light of new evidence.

In the Bayesian formula itself, a range was used for the chance of finding life on Mars. The same range was

used for the chance of abiotic gas production. The range used causes some potentially important edge cases to be overlooked. However, the largest part of the probability field lies within this range. The used range for $P(CH_4|nolife)$ was broader than used by Walker et al. [53] while still retaining its characteristics as a good bio-signature. The results are in line with the remarks of earlier work that methane is a viable bio-signature [7].

6

Conclusion and recommendations

6.1. Conclusions

This study aims to find the chance that Earth-like life was responsible for the methane spike around sol 305 (14th of June 2013), and express this in a percentage. Consequently, this study also aimed to explore what this form of life could be. These questions were investigated under the hypothesis, that life on Mars exists, and is similar to life on Earth. In order to facilitate the novel kinetic comparison of the Martian observation to known biotic methane production processes, the following investigative scheme was used. First the thermodynamic feasibility of catabolic reactions was explored. Secondly, the applicability of the kinetic model using experiments as ground truth was investigated. Following the applicability, the correlation of the kinetic model to Martian observations was found using an MC approach. Lastly, a Bayesian framework was constructed with the findings. This study provides a first quantification of biological probabilities compatible with the Bayesian framework for methane observations on Mars, and by extension similar rocky planets. The novel kinetic comparison effectively provided the Bayesian formula with data, resulting in the conclusions below. The results also show that this type of kinetic analysis can be performed on few and time-varied data points. The six used data points from the Martian observation were enough for this investigation, although more data points would allow for a more robust investigation.

6.1.1. Thermodynamic feasibility of catabolic reactions

Based on the thermodynamic calculations, methanogens and sulphate reducers could produce energy on current Mars. The thermodynamic analysis neglects phase changes of the water medium, but includes the thermodynamic effects of the low temperatures observed on the surface. The effect of micro-gravity on the substrate concentrations in the immediate surroundings of the microbes, differs per pathway. The trend is a light to moderate increase in Gibbs free energy without a fundamental change in temperature dependence. Reactions close to $-20[Kj/Mol]$ can become unlikely because of this minimum energy quantum. Methanogenesis and sulphate reduction are unaffected as their Gibbs free energies are very negative, and the effects of microgravity do not bring these reactions to the $-20[Kj/Mol]$ point. An important note here is that the micro-gravity assessment cannot quantify the gravity potential it uses, and that the gravity potential on Mars does not qualify as micro-gravity.

6.1.2. Applicability of the kinetic model using experiments as true positive

Based on the experiments on boom clay microbes in P-MRA and MAA conditions, biomass growth and sulfur gas levels develop dissimilar to the kinetic model. Therefore these cannot be used to compare the kinetic model to the Martian observations. The methane concentrations in the gas phase are within one standard deviation between the ADM1 simulations, earth conditions and MRA/MAA simulated Martian conditions. Therefore the methane product of the model can be compared to observations under Martian conditions. Other factors that likely impact Martian methane production were not investigated. These factors are discussed in chapter 2.2.2.

Table 6.1: Qualitative interpretation of the combined CH_4 and H_2S signals based on model findings. Observing any of the methane and hydrogen sulphide gas combinations is assumed to be equally likely under an abiotic system, and this chance is 'medium'. Table 6.1 shows the qualitative probability of observing 'C_i', which in the case of dynamic comparison is a significant correlation, assuming life exists or does not exist in the observed system.

C_i	$P(C_i\|life)$	$P(C_i\|nolife)$
CH4 and H2S	High	Medium
CH4 and no H2S	Low	Medium
No CH4 and H2S	Low	Medium
No CH4 and no H2S	Low	Medium

6.1.3. Kinetic model correlation to Martian observations

The kinetic ADM1 model had a two-tailed correlation p-value of at least 0.01 in 78% of the cases, with an average p-value of 0.094 ± 0.0012. This 0.78% is assumed to be the right input for the factor $P(CH_4|life)$ in the Bayesian framework. The dilution model gave stable distance results, but without an additional mass balance this method is purely indicative. The method showed that simple magnitude scaling could couple the observations to the model, independently from the Pearson correlation results. The results were produced using a Monte Carlo analysis where the input parameters of the ADM1 model were assumed to have a 33% standard deviation, from initial conditions, akin to Earthly wastewater. This deviation ensured that the input parameters never became negative while being able to come close to 0. The envisioned Martian conditions would only be a small subset of the used parameter space.

6.1.4. Constructing the Bayesian framework

The methane peak is a good biosignature based on Bayesian analysis. Being a good biosignature means that within the Bayesian formula 2.1 the posterior chance $P(life|CH_4)$ is larger than the prior probability $P(life)$, for any assumption of $P(CH_4|nolife)$. Based on thermodynamic calculations, experiments, and the ADM1 model, H_2S will be produced simultaneously if an anaerobic community is active on Mars. However, the current findings do not support a direct comparison between H_2S simulations from the ADM1 model and data observed on Mars. Quantified H_2S comparison between the model and observations would allow the Bayesian framework for anaerobic life, to be expanded, incorporating CH_4, H_2S and their individual and combined presence or absence. Positive detectability is defined as $\frac{P(Ci|life)}{P(Ci|nolife)} > 1$. Qualitatively this has been depicted in table 6.1. Positive detectability can be achieved with the combined methane hydrogen-sulfide signature.

6.2. Recommendations

Both the Pearson's correlation and dilution method neglects transport processes at this point. Assuming the community grows in the subsurface, soil transport processes, ice influence, and atmospheric transport are all effects that could influence gas detection. Analysing this can improve understanding of the effects these processes have on biosignature observability. It could show that subsurface growth kinetics are decoupled from the observations at the surface. This decoupling would disprove kinetic analysis as a method in this case.

The lack of an abiotic model defining $P(CH_4|nolife)$ generates much uncertainty. Experiments and simulations into abiotic methane production can constrain $P(CH_4|nolife)$ to a narrower range than the arbitrarily chosen range from 10% to 90% used in this study. Experiments combining the abiotic and biotic pathways could provide a list of production mechanisms that can systematically be ruled out or confirmed, thus further constraining $P(CH_4|nolife)$. These constraints allow the detectability of the potential biosignature to be assessed. Walker et al. [53] describes a statistical method using a Bernoulli distribution to infer whether further observations would increase or decrease confidence in biological presence based on this detectability [53]. Implementing this method to existing data could dictate the value of further research.

Analysing more methane peaks could improve trust in the found correlation not being a coincidence. Analysing the available Martian methane measurement database for more peaks can show if the correlation is only to this peak, or fits more peaks. Additionally, the SAM instrument of the Curiosity rover can detect sulphur gasses. Searching its data might show concurrent methane and sulphur peaks, providing data for the combined CH_4 and H_2S peak analysis. This combined analysis can produce combined signals that improve detectability as depicted in table: 6.1.

The bio-signature analysis can only indicate results. More certainty could be provided if the biological model were expanded. Temperature and phase change simulations can reduce uncertainty. To a lesser extent more chemical equilibria, organisms and micro-gravity effects do this too. Phase changes and temperature effects are likely to severely impact the functioning of the microbes and thus impact the correlation. Missing microbes like Methylotrophs that are a likely species from the Gibbs analysis, but are not represented in the ADM1 module also increase uncertainty. Additional Chemolithotrophic reactions should also be modelled, for example carboxydobacteria. These microbes dictate the gas production dynamics after hydrogen depletion. Soil matrix equilibria were not modelled, although these equilibria could have negatively impacted substrate availability and gas production via the formation of chemical complexes. Research into micro-gravity effects on communal kinetics would be needed to understand the types of effects that can be expected as only singular microbes have been researched instead of communities making it difficult to predict the expected gas production dynamics. Expanding the ADM1 model, or a new framework on all the points mentioned above, would improve the simulation data from indicative to predictive for more environments than just Mars.

Experimental data could replace simulated data in the kinetic analysis. This replacement can be achieved by measuring the gas composition over time in a simulated environment including temperature simulation. The experiments in this study only measured the gas composition at the end of the experiment. This is sufficient for model calibration, but not for direct correlation. An experiment with sufficient temporal resolution could replace the kinetic model. This experiment should be longer than eight days, improving the chances of finding delayed productivity. Ideally, it could keep gas pressure constant to simulate a connection to an atmosphere. Putting the resulting data into the correlation method would be no different from using the kinetic model, only with improved data reliability.

At this point a Pearson correlation in the MC context is used. An MCMC method (Markov Chain Monte Carlo) could provide a more accurate estimation of $P(CH_4|life)$ and its dependence on the input variables. Additionally, a clear idea of initial conditions can provide falsifiable environmental parameters that could be investigated in situ.

A

Code links

All of the code written for this study is available on Github. As are the experimental results.
Thermodynamic code: https://github.com/DylanDVerburg/GFEC
ADM1 Monte Carlo code: https://github.com/DylanDVerburg/ADM1_MRA
Experimental results: https://github.com/DylanDVerburg/Experimental-results/

B

Gibbs free energy code, exact values

Table B.1: Exact output for Hydrogenotrophic methanogenesis, figure: C.1a

For 4.0 * H2(g) + CO2(g) –> CH4(g) + 2.0 * H2O(l) :

Conc. red. [-]	H2(g)	CO2(g)	CH4(g)	H2O(l)	Gibbs(T)
0.0	1.000e-07	9.510e-01	1.000e-07	1.000e+03	9.276e-01 * T + -2.530e+02
0.2	8.000e-08	9.510e-01	1.050e-07	1.000e+03	9.355e-01 * T + -2.530e+02
0.4	6.000e-08	9.510e-01	1.100e-07	1.000e+03	9.454e-01 * T + -2.530e+02
0.6	4.000e-08	9.510e-01	1.150e-07	1.000e+03	9.593e-01 * T + -2.530e+02
0.8	2.000e-08	9.510e-01	1.200e-07	1.000e+03	9.827e-01 * T + -2.530e+02

Table B.2: Exact output for Formate based methylotrophic methanogenesis, figure: C.1b

For 4*HCO2-(aq) + 4*H+(aq) –> CH4(g) + 3*CO2(g) + 2*H2O(l) :

Conc. red. [-]	HCO2-(aq)	H+(aq)	CH4(g)	CO2(g)	H2O(l)	Gibbs(T)
0.0	1.000e+00	1.000e+00	1.000e-07	9.510e-01	1.000e+03	-6.277e-01 * T + -1.870e+02
0.2	8.000e-01	8.000e-01	5.000e-02	1.101e+00	1.000e+03	-5.001e-01 * T + -1.870e+02
0.4	6.000e-01	6.000e-01	1.000e-01	1.251e+00	1.000e+03	-4.720e-01 * T + -1.870e+02
0.6	4.000e-01	4.000e-01	1.500e-01	1.401e+00	1.000e+03	-4.388e-01 * T + -1.870e+02
0.8	2.000e-01	2.000e-01	2.000e-01	1.551e+00	1.000e+03	-3.878e-01 * T + -1.870e+02

Table B.3: Exact output for Hydrogen based methylotrophic methanogenesis, figure: C.1c

For CH3OH(l) + H2(g) –> CH4(g) + H2O(l) :

Conc. red. [-]	CH3OH(l)	H2(g)	CH4(g)	H2O(l)	Gibbs(T)
0.0	1.000e+00	1.000e-07	1.000e-07	1.000e+03	5.878e-02 * T + -1.220e+02
0.2	8.000e-01	1.000e-11	2.000e-01	1.000e+03	2.578e-01 * T + -1.220e+02
0.4	6.000e-01	1.000e-11	4.000e-01	1.000e+03	2.660e-01 * T + -1.220e+02
0.6	4.000e-01	1.000e-11	6.000e-01	1.001e+03	2.727e-01 * T + -1.220e+02
0.8	2.000e-01	1.000e-11	8.000e-01	1.001e+03	2.809e-01 * T + -1.220e+02

Table B.4: Exact output for Methylotrophic methanogenesis, figure: C.2a

For 4*CH3OH(l) –> CO2(g) + 3*CH4(g) + 2*H2O(l) :

Conc. red. [-]	CH3OH(l)	CO2(g)	CH4(g)	H2O(l)	Gibbs(T)
0.0	1.000e+00	9.510e-01	1.000e-07	1.000e+03	-6.925e-01 * T + -2.350e+02
0.2	8.000e-01	1.001e+00	1.500e-01	1.000e+03	-3.300e-01 * T + -2.350e+02
0.4	6.000e-01	1.051e+00	3.000e-01	1.000e+03	-3.027e-01 * T + -2.350e+02
0.6	4.000e-01	1.101e+00	4.500e-01	1.000e+03	-2.787e-01 * T + -2.350e+02
0.8	2.000e-01	1.151e+00	6.000e-01	1.000e+03	-2.481e-01 * T + -2.350e+02

Table B.5: Exact output for Aceticlastic methanogenesis, figure: C.2b

For CH3COOH(l) –> CO2(g) + CH4(g) :

Conc. red. [-]	CH3COOH(l)	CO2(g)	CH4(g)	Gibbs(T)
0.0	1.000e+00	9.510e-01	1.000e-07	-4.019e-01 * T + -1.913e+02
0.2	8.000e-01	1.151e+00	2.000e-01	-2.778e-01 * T + -1.913e+02
0.4	6.000e-01	1.351e+00	4.000e-01	-2.684e-01 * T + -1.913e+02
0.6	4.000e-01	1.551e+00	6.000e-01	-2.605e-01 * T + -1.913e+02
0.8	2.000e-01	1.751e+00	8.000e-01	-2.513e-01 * T + -1.913e+02

Table B.6: Exact output for Homoacetogenesis, figure: C.2c

For 4* CO2(g) + 8* H2(g) –>4* H2O(l) + 2* CH3COOH(l) :

Conc. red. [-]	CO2(g)	H2(g)	H2O(l)	CH3COOH(l)	Gibbs(T)
0.0	9.510e-01	1.000e-07	1.000e+03	1.000e+00	2.659e+00 * T + -1.232e+02
0.2	7.608e-01	1.000e-11	1.000e+03	1.095e+00	3.281e+00 * T + -1.232e+02
0.4	5.706e-01	1.000e-11	1.000e+03	1.190e+00	3.292e+00 * T + -1.232e+02
0.6	3.804e-01	1.000e-11	1.001e+03	1.285e+00	3.306e+00 * T + -1.232e+02
0.8	1.902e-01	1.000e-11	1.001e+03	1.380e+00	3.331e+00 * T + -1.232e+02

Table B.7: Exact output for Formaldyhyde based sulphate reduction to sulphur gas, figure: C.2d

For SO4-2(aq) + 2 * CH2O(aq) –> H2S(g) + 2*HCO3-(aq) :

Conc. red. [-]	SO4-2(aq)	CH2O(aq)	H2S(g)	HCO3-(aq)	Gibbs(T)
0.0	1.000e+00	1.000e+00	1.000e+00	1.000e+00	3.251e-01 * T + -7.256e+02
0.2	8.000e-01	6.000e-01	1.200e+00	1.400e+00	3.426e-01 * T + -7.256e+02
0.4	6.000e-01	2.000e-01	1.400e+00	1.800e+00	3.687e-01 * T + -7.256e+02
0.6	4.000e-01	1.000e-11	1.600e+00	2.200e+00	7.709e-01 * T + -7.256e+02
0.8	2.000e-01	1.000e-11	1.800e+00	2.600e+00	7.804e-01 * T + -7.256e+02

Table B.8: Exact output for Hydrogenotrophic sulfate reducers, figure: C.2e

For 5 * H2(g) + SO4-2(aq) –> H2S(g) + 4 * H2O(l) :

Conc. red. [-]	H2(g)	SO4-2(aq)	H2S(g)	H2O(l)	Gibbs(T)
0.0	1.000e-07	1.000e+00	1.000e+00	1.000e+03	9.576e-01 * T + -2.547e+02
0.2	8.000e-08	1.000e+00	1.000e+00	1.000e+03	9.668e-01 * T + -2.547e+02
0.4	6.000e-08	1.000e+00	1.000e+00	1.000e+03	9.788e-01 * T + -2.547e+02
0.6	4.000e-08	1.000e+00	1.000e+00	1.000e+03	9.956e-01 * T + -2.547e+02
0.8	2.000e-08	1.000e+00	1.000e+00	1.000e+03	1.024e+00 * T + -2.547e+02

C

Gibbs free energy images

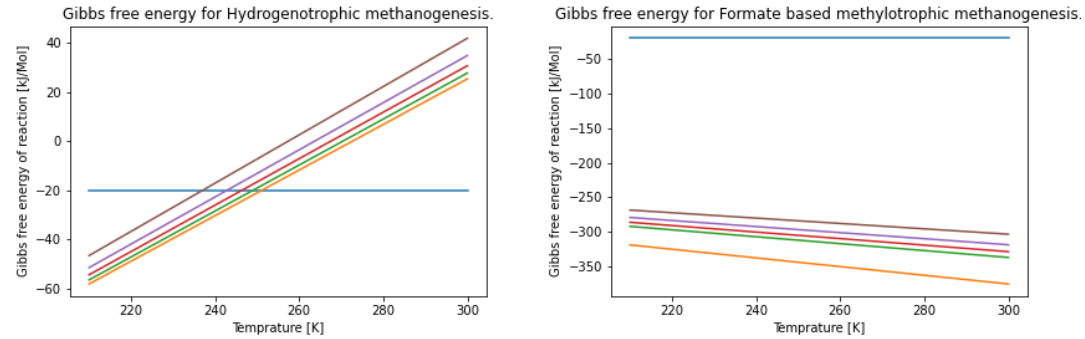

(a) (b)

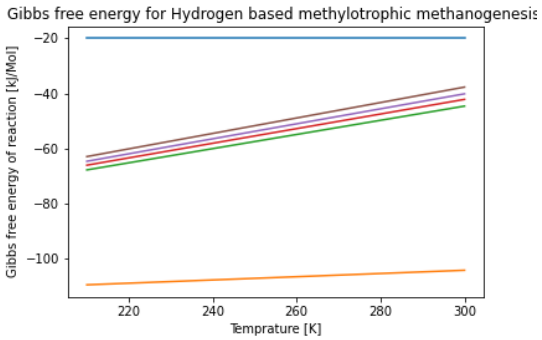

(c)

Figure C.1: Gibbs free energy for various red-ox reactions related to anaerobic communities, with a focus on Methanogenesis. The legend is consistent through all figures as is the temperature axis, which is based on Martian surface temperatures. Exact calculated numbers can be found in Appendix B. The reaction depicted in written in the graphs title.

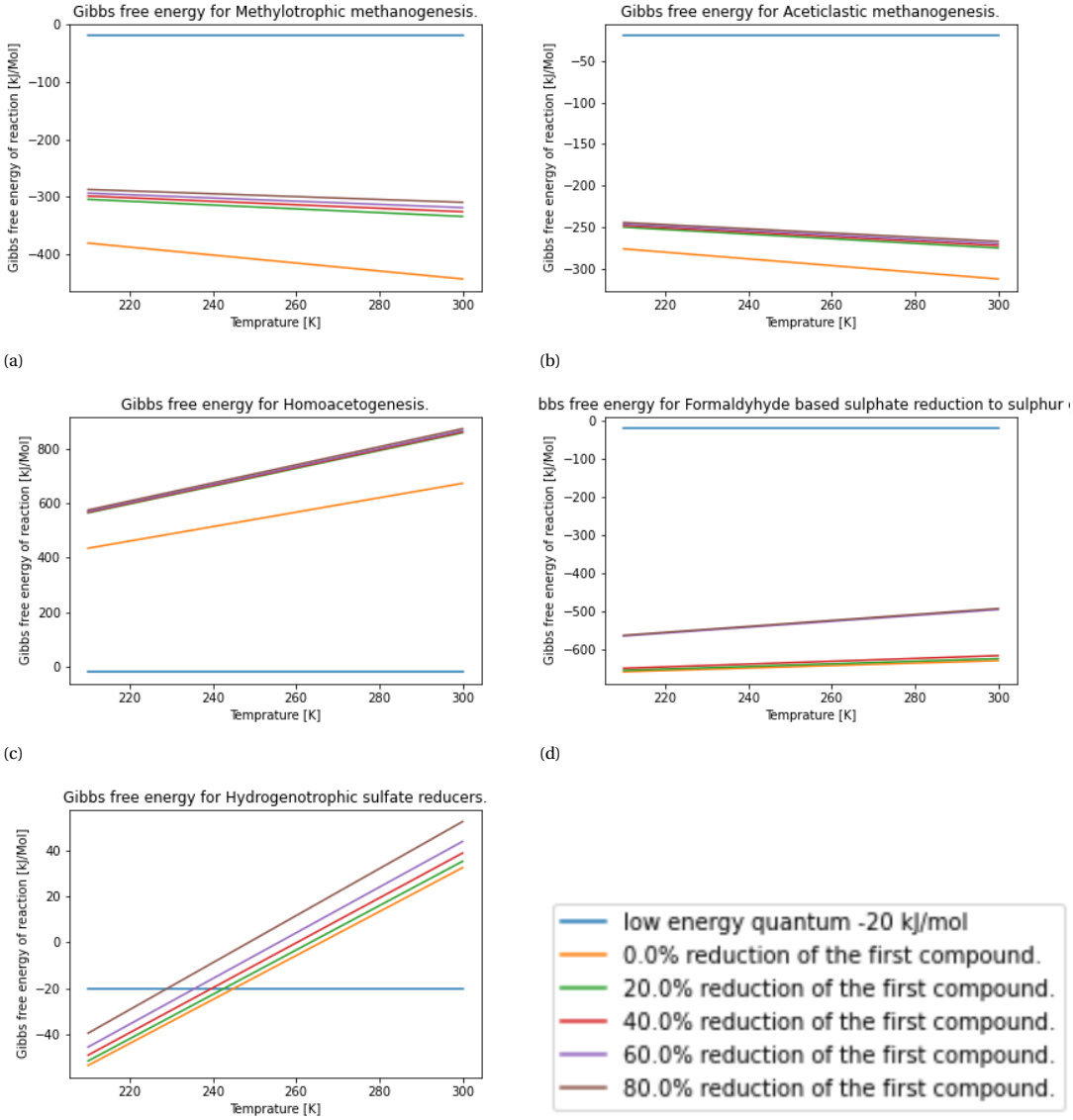

Figure C.2: Gibbs free energy for various red-ox reactions related to anaerobic communities, with a focus on Methanogenesis. The legend is consistent through all figures as is the temperature axis, which is based on Martian surface temperatures. Exact calculated numbers can be found in Appendix B. The reaction depicted in written in the graphs title.

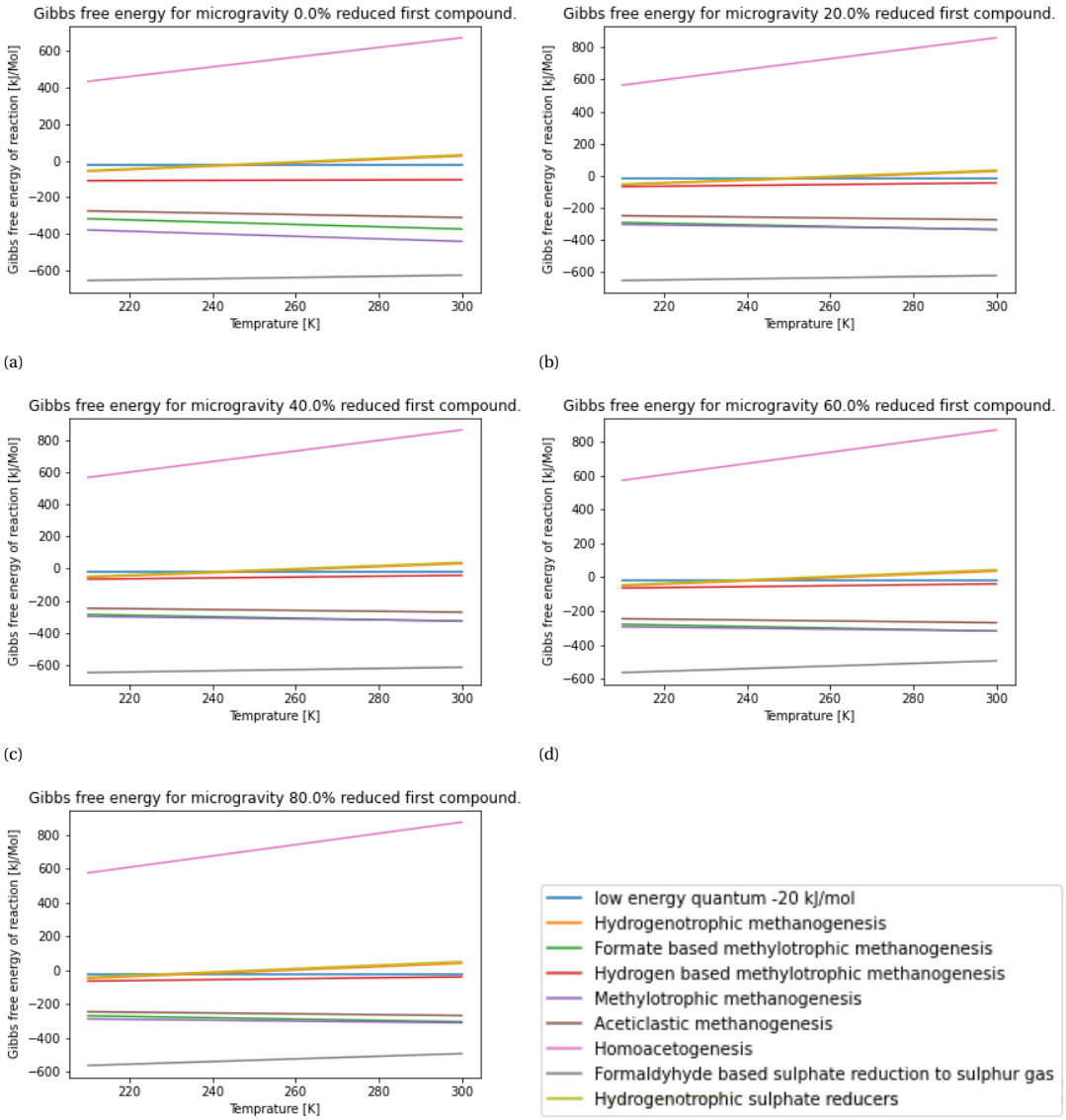

Figure C.3: Various graphs showing the theoretical effects of micro gravity on the microbial reactions, compared to each other. C.3a up to C.3e show this evolution. The legend in C.3f depicts the legend for all these graphs. As can be seen, a total restructure of the microbiome is not to be expected.

D

H2S measuring protocol

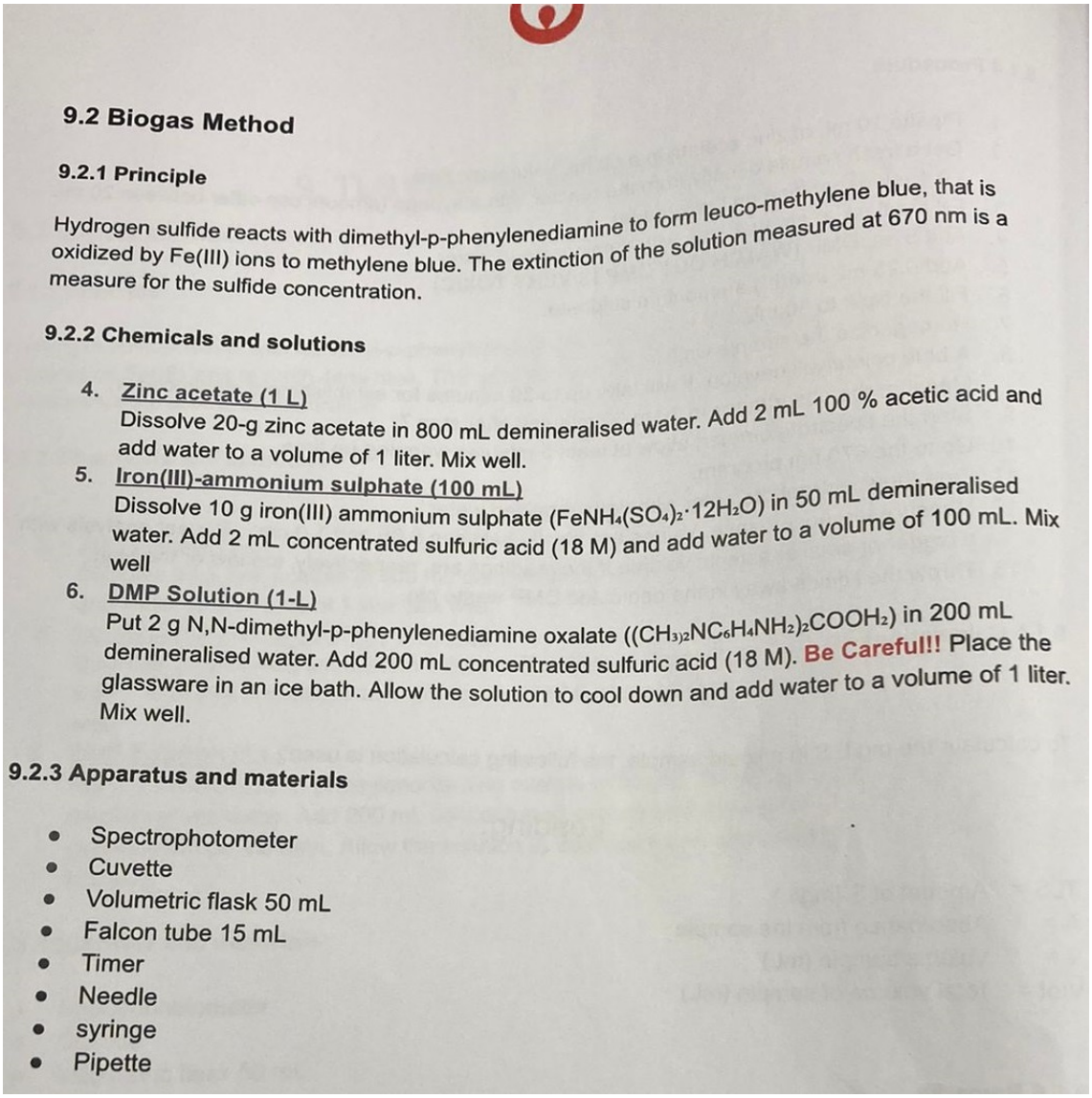

9.2 Biogas Method

9.2.1 Principle

Hydrogen sulfide reacts with dimethyl-p-phenylenediamine to form leuco-methylene blue, that is oxidized by Fe(III) ions to methylene blue. The extinction of the solution measured at 670 nm is a measure for the sulfide concentration.

9.2.2 Chemicals and solutions

4. Zinc acetate (1 L)
   Dissolve 20-g zinc acetate in 800 mL demineralised water. Add 2 mL 100 % acetic acid and add water to a volume of 1 liter. Mix well.
5. Iron(III)-ammonium sulphate (100 mL)
   Dissolve 10 g iron(III) ammonium sulphate ($FeNH_4(SO_4)_2 \cdot 12H_2O$) in 50 mL demineralised water. Add 2 mL concentrated sulfuric acid (18 M) and add water to a volume of 100 mL. Mix well
6. DMP Solution (1-L)
   Put 2 g N,N-dimethyl-p-phenylenediamine oxalate ($(CH_3)_2NC_6H_4NH_2)_2COOH_2$) in 200 mL demineralised water. Add 200 mL concentrated sulfuric acid (18 M). **Be Careful!!** Place the glassware in an ice bath. Allow the solution to cool down and add water to a volume of 1 liter. Mix well.

9.2.3 Apparatus and materials

- Spectrophotometer
- Cuvette
- Volumetric flask 50 mL
- Falcon tube 15 mL
- Timer
- Needle
- syringe
- Pipette

Figure D.1: First page of the internal Veolia H_2S measurement method. The method is used for measuring sulphur gas levels in the kinetic applicability stage of this document.

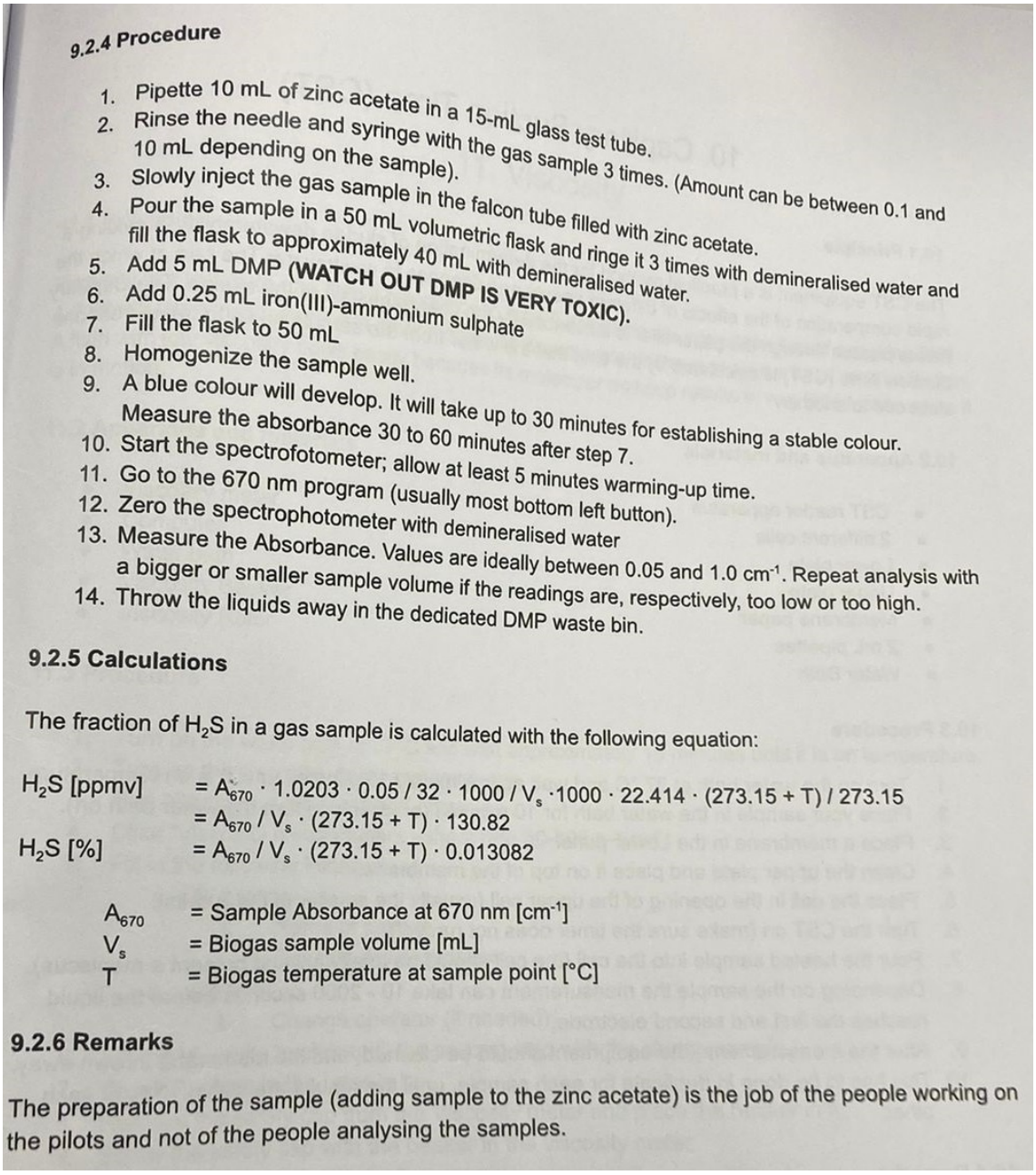

9.2.4 Procedure

1. Pipette 10 mL of zinc acetate in a 15-mL glass test tube.
2. Rinse the needle and syringe with the gas sample 3 times. (Amount can be between 0.1 and 10 mL depending on the sample).
3. Slowly inject the gas sample in the falcon tube filled with zinc acetate.
4. Pour the sample in a 50 mL volumetric flask and ringe it 3 times with demineralised water and fill the flask to approximately 40 mL with demineralised water.
5. Add 5 mL DMP (**WATCH OUT DMP IS VERY TOXIC).**
6. Add 0.25 mL iron(III)-ammonium sulphate
7. Fill the flask to 50 mL
8. Homogenize the sample well.
9. A blue colour will develop. It will take up to 30 minutes for establishing a stable colour. Measure the absorbance 30 to 60 minutes after step 7.
10. Start the spectrofotometer; allow at least 5 minutes warming-up time.
11. Go to the 670 nm program (usually most bottom left button).
12. Zero the spectrophotometer with demineralised water
13. Measure the Absorbance. Values are ideally between 0.05 and 1.0 cm^{-1}. Repeat analysis with a bigger or smaller sample volume if the readings are, respectively, too low or too high.
14. Throw the liquids away in the dedicated DMP waste bin.

9.2.5 Calculations

The fraction of H_2S in a gas sample is calculated with the following equation:

$$H_2S\ [ppmv] = A_{670} \cdot 1.0203 \cdot 0.05 / 32 \cdot 1000 / V_s \cdot 1000 \cdot 22.414 \cdot (273.15 + T) / 273.15$$
$$= A_{670} / V_s \cdot (273.15 + T) \cdot 130.82$$
$$H_2S\ [\%] = A_{670} / V_s \cdot (273.15 + T) \cdot 0.013082$$

A_{670} = Sample Absorbance at 670 nm [cm^{-1}]
V_s = Biogas sample volume [mL]
T = Biogas temperature at sample point [°C]

9.2.6 Remarks

The preparation of the sample (adding sample to the zinc acetate) is the job of the people working on the pilots and not of the people analysing the samples.

Figure D.2: Second page of the internal Veolia H_2S measurement method. The method is used for measuring sulphur gas levels in the kinetic applicability stage of this document.

Bibliography

[1] Michael Blaut. Metabolism of methanogens. *Antonie van Leeuwenhoek 1994 66:1*, 66(1):187–208, mar 1994. ISSN 1572-9699. doi: 10.1007/BF00871639. URL https://link-springer-com.tudelft.idm.oclc.org/article/10.1007/BF00871639.

[2] Benedict Borer, Joaquin Jimenez-Martinez, Roman Stocker, and Dani Or. Reduced gravity promotes bacterially mediated anoxic hotspots in unsaturated porous media. *Scientific Reports*, 2020. ISSN 20452322. doi: 10.1038/s41598-020-65362-w.

[3] C. S. Boxe, K. P. Hand, K. H. Nealson, Y. L. Yung, and A. Saiz-Lopez. An active nitrogen cycle on Mars sufficient to support a subsurface biosphere. *International Journal of Astrobiology*, 2012. ISSN 14735504. doi: 10.1017/S1473550411000401.

[4] Jennifer Buz, Bethany L. Ehlmann, Lu Pan, and John P. Grotzinger. Mineralogy and stratigraphy of the Gale crater rim, wall, and floor units. *Journal of Geophysical Research: Planets*, 2017. ISSN 21699100. doi: 10.1002/2016JE005163.

[5] Xiaobin Cao, Huiming Bao, and Yongbo Peng. A kinetic model for isotopologue signatures of methane generated by biotic and abiotic CO 2 methanation. *Geochimica et Cosmochimica Acta*, 2019. ISSN 00167037. doi: 10.1016/j.gca.2019.01.021.

[6] John Carter, Lucie Riu, François Poulet, Jean-Pierre Bibring, Yves Langevin, and Brigitte Gondet. A Mars Orbital Catalog of Aqueous Alteration Signatures (MOCAAS). 2022. doi: 10.1016/j.icarus.2022.115164. URL https://doi.org/10.1016/j.icarus.2022.115164.

[7] David C. Catling, Joshua Krissansen-Totton, Nancy Y. Kiang, David Crisp, Tyler D. Robinson, Shiladitya Dassarma, Andrew J. Rushby, Anthony Del Genio, William Bains, and Shawn Domagal-Goldman. Exoplanet Biosignatures: A Framework for Their Assessment. *Astrobiology*, 18(6):709–738, jun 2018. ISSN 15311074. doi: 10.1089/AST.2017.1737/ASSET/IMAGES/LARGE/FIGURE2.JPEG. URL https://www-liebertpub-com.tudelft.idm.oclc.org/doi/10.1089/ast.2017.1737.

[8] Pamela Ceron-Chafla, Yu Ting Chang, Korneel Rabaey, Jules B. van Lier, and Ralph E.F. Lindeboom. Directional Selection of Microbial Community Reduces Propionate Accumulation in Glycerol and Glucose Anaerobic Bioconversion Under Elevated pCO2. *Frontiers in Microbiology*, 12:1583, jun 2021. ISSN 1664302X. doi: 10.3389/fmicb.2021.675763.

[9] Vladimir S. Cheptsov, Elena A. Vorobyova, George A. Osipov, Natalia A. Manucharova, Lubov' M. Polyanskaya, Mikhail V. Gorlenko, Anatoli K. Pavlov, Marina S. Rosanova, and Vladimir N. Lomasov. Microbial activity in martian analog soils after ionizing radiation: Implications for the preservation of subsurface life on mars. *AIMS Microbiology*, 2018. ISSN 24711888. doi: 10.3934/microbiol.2018.3.541.

[10] Svatopluk Civiš and Antonín Knížek. Abiotic Formation of Methane and Prebiotic Molecules on Mars and Other Planets. *ACS Earth and Space Chemistry*, 5(5):1172–1179, may 2021. ISSN 24723452. doi: 10.1021/ACSEARTHSPACECHEM.1C00041/ASSET/IMAGES/MEDIUM/SP1C00041_M007.GIF. URL https://pubs-acs-org.tudelft.idm.oclc.org/doi/full/10.1021/acsearthspacechem.1c00041.

[11] R. E. Davies. Panspermia: Unlikely, unsupported, but just possible. *Acta Astronautica*, 17(1):129–135, jan 1988. ISSN 0094-5765. doi: 10.1016/0094-5765(88)90136-1.

[12] John A. Dean. *Lange's Handbook of Chemistry, Fifteenth Edition*. McGraw- Hill Inc., 1999. ISBN 0-07-016384-7. URL http://fptl.ru/biblioteka/spravo4niki/dean.pdf%5Cnhttp://journals.lww.com/soilsci/Abstract/1944/07000/Handbook_of_Chemistry.13.aspx.

[13] Kumulative Dissertation and Janosch Schirmack Berlin. Activity of methanogenic archaea under simulated Mars analog conditions. 2014. URL http://publishup.uni-potsdam.de/opus4-ubp/frontdoor/index/index/docId/7301.

[14] NASA's Jet Propulsion Laboratory Earth Science Communications Team. Carbon Dioxide | Vital Signs – Climate Change: Vital Signs of the Planet. URL https://climate.nasa.gov/vital-signs/carbon-dioxide/.

[15] D H Ehhalt and U Schmidt. Sources and Sinks of Atmospheric Methane. 116, 1978.

[16] Michael E. Essington. *Soil and Water Chemistry: An Integrative Approach*. 2 edition, 2003. ISBN 978-1032098692.

[17] Giuseppe Etiope and Barbara Sherwood Lollar. Abiotic methane on earth. *Reviews of Geophysics*, 51(2): 276–299, jun 2013. ISSN 19449208. doi: 10.1002/ROG.20011.

[18] S. Franck, A. Block, W. Von Bloh, C. Bounama, H. J. Schellnhuber, and Y. Svirezhev. Habitable zone for Earth-like planets in the solar system. *Planetary and Space Science*, 48(11):1099–1105, sep 2000. ISSN 0032-0633. doi: 10.1016/S0032-0633(00)00084-2.

[19] M. Frederickx, L., De Craen, M., Honty. *An advanced mineralogical study of the clay mineral fraction in Boom Clay*. PhD thesis, KUL - Katholieke Universiteit Leuven., 2020.

[20] German Collection of Microorganisms and Cell Cultures GmbH. List of Media for Microorganisms: 141c METHANOCOCCOIDES MEDIUM. URL https://www.dsmz.de/collection/catalogue/microorganisms/culture-technology/list-of-media-for-microorganisms.

[21] Marco Giuranna, Sébastien Viscardy, Frank Daerden, Lori Neary, Giuseppe Etiope, Dorothy Oehler, Vittorio Formisano, Alessandro Aronica, Paulina Wolkenberg, Shohei Aoki, Alejandro Cardesín-Moinelo, Julia Marín-Yaseli de la Parra, Donald Merritt, and Marilena Amoroso. Independent confirmation of a methane spike on Mars and a source region east of Gale Crater. *Nature Geoscience*, 2019. ISSN 17520908. doi: 10.1038/s41561-019-0331-9.

[22] Donald M. Hassler, Cary Zeitlin, Robert F. Wimmer-Schweingruber, Bent Ehresmann, Scot Rafkin, Jennifer L. Eigenbrode, David E. Brinza, Gerald Weigle, Stephan Böttcher, Eckart Böhm, Soenke Burmeister, Jingnan Guo, Jan Köhler, Cesar Martin, Guenther Reitz, Francis A. Cucinotta, Myung Hee Kim, David Grinspoon, Mark A. Bullock, Arik Posner, Javier Gómez-Elvira, Ashwin Vasavada, and John P. Grotzinger. Mars' surface radiation environment measured with the Mars science laboratory's curiosity rover. *Science*, 343(6169), jan 2014. ISSN 10959203. doi: 10.1126/SCIENCE.1244797/SUPPL_FILE/HASSLER.SM.PDF. URL https://www-science-org.tudelft.idm.oclc.org/doi/abs/10.1126/science.1244797.

[23] C. Hirt, S. J. Claessens, M. Kuhn, and W. E. Featherstone. Kilometer-resolution gravity field of Mars: MGM2011. *Planetary and Space Science*, 67(1):147–154, jul 2012. ISSN 00320633. doi: 10.1016/j.pss.2012.02.006.

[24] Kohei Ino, Alex W. Hernsdorf, Uta Konno, Mariko Kouduka, Katsunori Yanagawa, Shingo Kato, Michinari Sunamura, Akinari Hirota, Yoko S. Togo, Kazumasa Ito, Akari Fukuda, Teruki Iwatsuki, Takashi Mizuno, Daisuke D. Komatsu, Urumu Tsunogai, Toyoho Ishimura, Yuki Amano, Brian C. Thomas, Jillian F. Banfield, and Yohey Suzuki. Ecological and genomic profiling of anaerobic methane-oxidizing archaea in a deep granitic environment. *The ISME Journal 2018 12:1*, 12(1):31–47, sep 2017. ISSN 1751-7370. doi: 10.1038/ISMEJ.2017.140. URL https://www-nature-com.tudelft.idm.oclc.org/articles/ismej2017140.

[25] F. Javier Martín-Torres, María Paz Zorzano, Patricia Valentín-Serrano, Ari Matti Harri, Maria Genzer, Osku Kemppinen, Edgard G. Rivera-Valentin, Insoo Jun, James Wray, Morten Bo Madsen, Walter Goetz, Alfred S. McEwen, Craig Hardgrove, Nilton Renno, Vincent F. Chevrier, Michael Mischna, Rafael Navarro-González, Jesús Martínez-Frías, Pamela Conrad, Tim McConnochie, Charles Cockell, Gilles Berger, Ashwin R. Vasavada, Dawn Sumner, and David Vaniman. Transient liquid water and water activity at Gale crater on Mars. *Nature Geoscience 2014 8:5*, 8(5):357–361, apr 2015. ISSN 1752-0908. doi: 10.1038/NGEO2412. URL https://www-nature-com.tudelft.idm.oclc.org/articles/ngeo2412.

[26] S J.W.H. Sulfate reduction in methanogenic bioreactors. *FEMS Microbiology Reviews*, 15(2-3):119–136, oct 1994. ISSN 01686445. doi: 10.1016/0168-6445(94)90108-2.

[27] Timothy A. Kral and S. Travis Aitheide. Methanogen survival following exposure to desiccation, low pressure and martian regolith analogs. *Planetary and Space Science*, 89:167–171, dec 2013. ISSN 0032-0633. doi: 10.1016/J.PSS.2013.09.010.

[28] Timothy A. Kral, Curtis R. Bekkum, and Christopher P. McKay. Growth of methanogens on a mars soil simulant. *Origins of Life and Evolution of the Biosphere*, 2004. ISSN 01696149. doi: 10.1023/B:ORIG.0000043129.68196.5f.

[29] Vladimir A. Krasnopolsky. Some problems related to the origin of methane on Mars. *Icarus*, 2006. ISSN 00191035. doi: 10.1016/j.icarus.2005.10.015.

[30] Vladimir A Krasnopolsky, Jean Pierre Maillard, and Tobias C Owen. Detection of methane in the martian atmosphere: Evidence for life? *Icarus*, 172(2):537–547, 2004. ISSN 00191035. doi: 10.1016/j.icarus.2004.07.004. URL www.elsevier.com/locate/icarus.

[31] Guillaume Lamarche-Gagnon, Raven Comery, Charles W. Greer, and Lyle G Whyte. Evidence of in situ microbial activity and sulphidogenesis in perennially sub-0 °C and hypersaline sediments of a high Arctic permafrost spring. *Extremophiles*, 19(1):1–15, 2015. ISSN 14334909. doi: 10.1007/s00792-014-0703-4.

[32] Franck Lefèvre and François Forget. Observed variations of methane on Mars unexplained by known atmospheric chemistry and physics. *Nature 2009 460:7256*, 460(7256):720–723, aug 2009. ISSN 1476-4687. doi: 10.1038/NATURE08228. URL https://www-nature-com.tudelft.idm.oclc.org/articles/nature08228.

[33] J. M.T. Lewis, J. L. Eigenbrode, G. M. Wong, A. C. McAdam, P. D. Archer, B. Sutter, M. Millan, R. H. Williams, M. Guzman, A. Das, E. B. Rampe, C. N. Achilles, H. B. Franz, S. Andrejkovičová, C. A. Knudson, and P. R. Mahaffy. Pyrolysis of Oxalate, Acetate, and Perchlorate Mixtures and the Implications for Organic Salts on Mars. *Journal of Geophysical Research: Planets*, 2021. ISSN 21699100. doi: 10.1029/2020JE006803.

[34] Ralph E.F. Lindeboom, Ivet Ferrer, Jan Weijma, and Jules B. van Lier. Effect of substrate and cation requirement on anaerobic volatile fatty acid conversion rates at elevated biogas pressure. *Bioresource Technology*, 150:60–66, dec 2013. ISSN 0960-8524. doi: 10.1016/J.BIORTECH.2013.09.100.

[35] William Martin, John Baross, Deborah Kelley, and Michael J. Russell. Hydrothermal vents and the origin of life, sep 2008. ISSN 17401526. URL https://www-nature-com.tudelft.idm.oclc.org/articles/nrmicro1991.

[36] Deborah Maus, Jacob Heinz, Janosch Schirmack, Alessandro Airo, Samuel P. Kounaves, Dirk Wagner, and Dirk Schulze-Makuch. Methanogenic Archaea Can Produce Methane in Deliquescence-Driven Mars Analog Environments. *Scientific Reports*, 2020. ISSN 20452322. doi: 10.1038/s41598-019-56267-4.

[37] R. L. Mickol, Y. A. Takagi, and T. A. Kral. Survival of non-psychrophilic methanogens exposed to martian diurnal and 48-h temperature cycles. *Planetary and Space Science*, 157:63–71, aug 2018. ISSN 0032-0633. doi: 10.1016/J.PSS.2018.03.012.

[38] Volker Müller and Verena Hess. The Minimum Biological Energy Quantum. *Frontiers in Microbiology*, 8(OCT), oct 2017. ISSN 1664302X. doi: 10.3389/FMICB.2017.02019. URL /pmc/articles/PMC5662883//pmc/articles/PMC5662883/?report=abstracthttps://www-ncbi-nlm-nih-gov.tudelft.idm.oclc.org/pmc/articles/PMC5662883/.

[39] Luong N. Nguyen, Anh Q. Nguyen, and Long D. Nghiem. Microbial Community in Anaerobic Digestion System: Progression in Microbial Ecology. In *Energy, Environment, and Sustainability*. 2019. doi: 10.1007/978-981-13-3259-3_15.

[40] Cheryl A. Nickerson, C. Mark Ott, James W. Wilson, Rajee Ramamurthy, and Duane L. Pierson. Microbial Responses to Microgravity and Other Low-Shear Environments. *Microbiology and Molecular Biology Reviews*, 68(2):345–361, jun 2004. ISSN 1092-2172. doi: 10.1128/mmbr.68.2.345-361.2004. URL https://journals-asm-org.tudelft.idm.oclc.org/doi/abs/10.1128/MMBR.68.2.345-361.2004.

[41] I. N. Reid, W. B. Sparks, S. Lubow, M. McGrath, M. Livio, J. Valenti, K. R. Sowers, H. D. Shukla, S. MacAuley, T. Miller, R. Suvanasuthi, R. Belas, A. Colman, F. T. Robb, P. DasSarma, J. A. Müller, J. A. Coker, R. Cavicchioli, F. Chen, and S. DasSarma. Terrestrial models for extraterrestrial life: methanogens and halophiles at Martian temperatures. *International Journal of Astrobiology*, 5(2):89–97, apr 2006. ISSN 1475-3006. doi: 10.1017/S1473550406002916. URL https://www-cambridge-org.tudelft.idm.oclc.org/core/journals/international-journal-of-astrobiology/article/terrestrial-models-for-extraterrestrial-life-methanogens-and-halophiles-at-martian-temperatures00977AD940A322D6BB9ADCB55FF7E161.

[42] Christian Rosén, Ulf Jeppsson, and Christian Rosen. Aspects on ADM1 Implementation within the BSM2 Framework. 2006.

[43] P Sadrimajd, P Mannion, E Howley, and P N L Lens. PyADM1: a Python implementation of Anaerobic Digestion Model No. 1. *bioRxiv*, page 2021.03.03.433746, 2021. doi: 10.1101/2021.03.03.433746. URL https://doi.org/10.1101/2021.03.03.433746https://www.biorxiv.org/content/10.1101/2021.03.03.433746v1%0Ahttps://www.biorxiv.org/content/10.1101/2021.03.03.433746v1.abstract.

[44] Edward W. Schwieterman, Nancy Y. Kiang, Mary N. Parenteau, Chester E. Harman, Shiladitya Dassarma, Theresa M. Fisher, Giada N. Arney, Hilairy E. Hartnett, Christopher T. Reinhard, Stephanie L. Olson, Victoria S. Meadows, Charles S. Cockell, Sara I. Walker, John Lee Grenfell, Siddharth Hegde, Sarah Rugheimer, Renyu Hu, and Timothy W. Lyons. Exoplanet Biosignatures: A Review of Remotely Detectable Signs of Life, 2018. ISSN 15311074.

[45] Navita Sinha and Timothy A. Kral. Effect of uvc radiation on hydrated and desiccated cultures of slightly halophilic and non-halophilic methanogenic archaea: Implications for life on mars. *Microorganisms*, 2018. ISSN 20762607. doi: 10.3390/microorganisms6020043.

[46] Navita Sinha, Sudip Nepal, Timothy Kral, and Pradeep Kumar. Survivability and growth kinetics of methanogenic archaea at various pHs and pressures: Implications for deep subsurface life on Mars. 2016. doi: 10.1016/j.pss.2016.11.012. URL http://dx.doi.org/10.1016/j.pss.2016.11.012.

[47] Kimberly Solon. IWA Anaerobic Digestion Model No. 1 extended with Phosphorus and Sulfur Literature Review extended with Phosphorus and Sulfur LITERATURE REVIEW. 2015.

[48] Jennifer C. Stern, Brad Sutter, W. Andrew Jackson, Rafael Navarro-González, Christopher P. McKay, Douglas W. Ming, P. Douglas Archer, and Paul R. Mahaffy. The nitrate/(per)chlorate relationship on Mars. *Geophysical Research Letters*, 2017. ISSN 19448007. doi: 10.1002/2016GL072199.

[49] J. D. Tarnas, J. F. Mustard, B. Sherwood Lollar, M. S. Bramble, K. M. Cannon, A. M. Palumbo, and A. C. Plesa. Radiolytic H2 production on Noachian Mars: Implications for habitability and atmospheric warming. *Earth and Planetary Science Letters*, 2018. ISSN 0012821X. doi: 10.1016/j.epsl.2018.09.001.

[50] Gary F Teletzke, H Ted Davis, and Le Scriven. CHEMICAL ENGINEERING COMMUNICATIONS HOW LIQUIDS SPREAD ON SOLIDS. *CHEMICAL ENGINEERING COMMUNICATIONS*, 55:41–82, 1987. ISSN 1563-5201. doi: 10.1080/00986448708911919. URL https://www.tandfonline.com/action/journalInformation?journalCode=gcec20.

[51] M. L. Teske, A., Dhillon, A., Sogin. Genomic Markers of Ancient Anaerobic Microbial Pathways: Sulfate Reduction, Methanogenesis, and Methane Oxidation. *The Biological Bulletin*, 204(2):186–191, 2003.

[52] Melissa G. Trainer, Michael H. Wong, Timothy H. McConnochie, Heather B. Franz, Sushil K. Atreya, Pamela G. Conrad, Franck Lefèvre, Paul R. Mahaffy, Charles A. Malespin, Heidi L.K. Manning, Javier Martín-Torres, Germán M. Martínez, Christopher P. McKay, Rafael Navarro-González, Álvaro Vicente-Retortillo, Christopher R. Webster, and María Paz Zorzano. Seasonal Variations in Atmospheric Composition as Measured in Gale Crater, Mars. *Journal of Geophysical Research: Planets*, 124(11):3000–3024, nov 2019. ISSN 21699100. doi: 10.1029/2019JE006175.

[53] Sara I. Walker, William Bains, Leroy Cronin, Shiladitya Dassarma, Sebastian Danielache, Shawn Domagal-Goldman, Betul Kacar, Nancy Y. Kiang, Adrian Lenardic, Christopher T. Reinhard, William Moore, Edward W. Schwieterman, Evgenya L. Shkolnik, and Harrison B. Smith. Exoplanet Biosignatures: Future Directions. *Astrobiology*, 2018. ISSN 15311074. doi: 10.1089/ast.2017.1738.

[54] Christopher R. Webster, Paul R. Mahaffy, Sushil K. Atreya, John E. Moores, Gregory J. Flesch, Charles Malespin, Christopher P. McKay, German Martinez, Christina L. Smith, Javier Martin-Torres, Javier Gomez-Elvira, Maria Paz Zorzano, Michael H. Wong, Melissa G. Trainer, Andrew Steele, Doug Archer, Brad Sutter, Patrice J. Coll, Caroline Freissinet, Pierre Yves Meslin, Raina V. Gough, Christopher H. House, Alexander Pavlov, Jennifer L. Eigenbrode, Daniel P. Glavin, John C. Pearson, Didier Keymeulen, Lance E. Christensen, Susanne P. Schwenzer, Rafael Navarro-Gonzalez, Jorge Pla-García, Scot C.R. Rafkin, Álvaro Vicente-Retortillo, Henrik Kahanpää, Daniel Viudez-Moreiras, Michael D. Smith, Ari Matti Harri, Maria Genzer, Donald M. Hassler, Mark Lemmon, Joy Crisp, Stanley P. Sander, Richard W. Zurek, and Ashwin R. Vasavada. Background levels of methane in Mars' atmosphere show strong seasonal variations. *Science*, 360(6393):1093–1096, 2018. ISSN 10959203. doi: 10.1126/science.aaq0131. URL `https://www.science.org`.

[55] Christopher R. Webster, Paul R. Mahaffy, Jorge Pla-Garcia, Scot C.R. Rafkin, John E. Moores, Sushil K. Atreya, Gregory J. Flesch, Charles A. Malespin, Samuel M. Teinturier, Hemani Kalucha, Christina L. Smith, Daniel Viúdez-Moreiras, and Ashwin R. Vasavada. Day-night differences in Mars methane suggest nighttime containment at Gale crater. *Astronomy and Astrophysics*, 2021. ISSN 14320746. doi: 10.1051/0004-6361/202040030.

[56] Zhen Ya Zhang and Takaaki Maekawa. Effects of sulfur-containing compounds on the growth and methane production of acclimated-mixed methanogens. *Biomass and Bioenergy*, 1996. ISSN 09619534. doi: 10.1016/0961-9534(95)00054-2.